

**3rd IAA Conference on Space Situational Awareness (ICSSA)
Madrid, Spain**

**IAA-ICSSA-22-0X-XX
RUSSIAN ASAT DEBRIS CLOUD EVOLUTION AND RISK**

**Daniel Oltrogge⁽¹⁾, Salvatore Alfano⁽²⁾, David Vallado⁽³⁾,
Pete Zimmer⁽⁴⁾, Robert Hall⁽⁵⁾, Jim Wilson⁽⁶⁾, Mike Siegers⁽⁷⁾, Joshua Aurich⁽⁸⁾**

⁽¹⁾ COMSPOC Corporation, 5040 Cliff Pt Cir E, Colorado Springs, CO 80919,
+1(719)482-4552, dan@comspoc.com

⁽²⁾ COMSPOC Corporation, 86 N Sherwood Glen, Monument CO 80132,
+1(719)487-9844, salfano@comspoc.com

⁽³⁾ COMSPOC Corporation, 16835 Horizon Ridge Trail, Colorado Springs, CO 80908,
U.S.A., +1(719)-330-3517, dvallado@comspoc.com

⁽⁴⁾ J.T. McGraw and Associates LLC, Placitas, NM 87043 U.S.A., zimm@lodestar.org

⁽⁵⁾ COMSPOC Corporation, 220 Valley Creed Drive, Exton, PA 19341 U.S.A.,
+1(610)564-9669, rhall@comspoc.com

⁽⁶⁾ COMSPOC Corporation, 220 Valley Creed Drive, Exton, PA 19341 U.S.A.,
+1(484)432-4269, jwilson@comspoc.com

⁽⁷⁾ Planet, 645 Harrison Street, San Francisco, CA 94107 U.S.A.,
mike.siegers@planet.com

⁽⁸⁾ Planet, 645 Harrison Street, San Francisco, CA 94107 U.S.A.,
joshua.aurich@planet.com

Keywords: LEO, Russian ASAT test, constellation, conjunction squall, collision

In this paper, we analyze the Russian ASAT intercept of the COSMOS 1408 spacecraft that occurred 15 November 2021, using published NOTAMs and public orbit and spacecraft data to infer the likely ASAT engagement scenario employed. That scenario is then used to infer imparted velocity directions and magnitudes. Two independent breakup models (one discrete “representative scenario” model and one continuum model) were then employed to determine where generated COSMOS 1408 debris fragments were likely to go, what satellites would be affected, and how operator workloads would be changed because of the test. Results indicate that debris fragments do pose a collision risk to Low Earth Orbit (LEO) spacecraft, especially spacecraft in sun-synchronous orbits (e.g., Earth-observing), very large spacecraft (notably, the International Space Station or ISS), and large constellations (for example, the Starlink constellation). The corresponding increases in close approach and collision warnings, accompanied by increases in avoidance maneuvers required for flight safety, will place a burden on operators for approximately 1.5 years after the intercept occurred.

1. Introduction

On November 15, 2021, Russia conducted an ASAT test, launching an ASAT weapon system to intercept and destroy the on-orbit COMOS 1408, a defunct Soviet Tselina-D family of Electronic Intelligence (ELINT) satellites [1, 2, 3] that was launched on 16 September 1982 into an 82.5° inclined, roughly 540 km circular orbit.

2. Test details inferred from public data sources

The Russians launched a Nudol ASAT weapon system [4] from Plesetsk Cosmodrome. Its target was COSMOS 1408, reportedly a dead Soviet-era ELINT spacecraft launched in 1982. The pre-intercept mass of COSMOS 1408 was estimated to be 2108 kg [5].

2.1. Optical tracking of COSMOS 1408 debris fragments

The first reports of the ASAT test spread around social media around 1200 UTC on November 15. The first available twilight pass over a COMSPOC optical system was at 1800 UTC over eastern Australia. The optical system there was able to image the pass, as shown in **Figure 1**, detecting four pieces of debris in a roughly 10 x 20 km area around the last published TLE position. The brightest fragment, with average GAIA g-band magnitude of 9.2, is also the closest to the parent TLE position and is estimated to be roughly 1.5 m² assuming standard optical properties and accounting for slant range. The other bright piece is magnitude 9.5, so also meter-scale, while the two smaller pieces are magnitude 12.6 and 13 and therefore ≈0.5m in size. Unsurprisingly, all pieces show significant variability associated with tumbling.

Because the parent orbit was nearly Sun-synchronous, the debris field presented only a few twilight observation opportunities before precessing into a largely inaccessible orientation for optical observations. Thus, these are the only multi-object detections we were able to obtain.

2.2. Estimating the intercept time

A key step when developing the intercept scenario is to estimate when the intercept occurred. Starting with the pre-intercept orbital information for the ASAT's target, Cosmos 1408 (Satellite number 13552 in the space-track.org Satellite Catalog [6], we performed subsequent analysis to determine the debris origin point (corresponding to the impact time). Sampling at a prescribed step size over the span of the analysis (initially once per minute over 8 hours and then a tenth of a second interval in a 5-minute span), the out-of-plane distance and radial (as a proxy for in-plane) separation for each piece of debris was assessed relative to the parent (pre-collision) TLE position. An overall distance measurement was then computed as the square root of the sum of the squares of these two distances.

Realizing the initial orbit determinations following a breakup event can involve significant uncertainty, we selected only those pieces that came within 0.25km cross-track and 3 km radially of the parent satellite. **Figure 2** shows the cross-track component history for 76 cataloged debris pieces out of the initial 185 fragments published on Space-Track [6] in the first tranche released two weeks after the incident. To develop a representative intercept scenario, the orbits of tracked debris fragments were then propagated backwards until they came together. As shown, compiling these distances produced a common minimum point corresponding to the impact time which as estimated using this approach to be 15 Nov 2021 at 02:47:31.5 UTC.

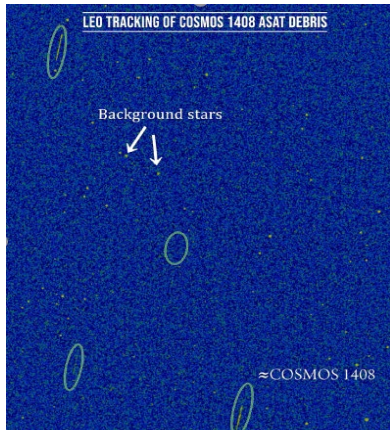


Figure 1: Optical tracking of COSMOS 1408 debris.

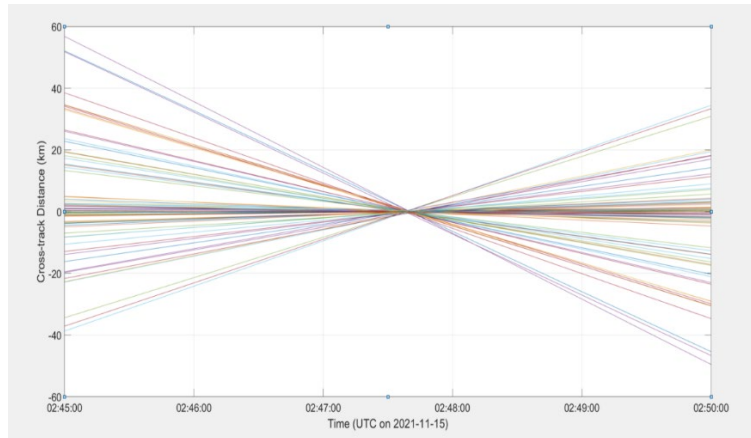


Figure 2: Estimation of intercept time (and therefore location)

2.3. Inferring spread velocities at intercept

After a collision, it can take many years to fully associate and catalog debris fragments from the event. State vectors and ephemerides are released over an extended period of time, sometimes years. The orbit conditions of newly tracked objects are analyzed to determine which launches, fragmentation events, boosters, upper stages, or spacecraft they likely came from. Determining a definitive set of object state vectors for all debris fragments is therefore a nontrivial task. Looking back through the historical dataset often provides new insights whereby the initially tracked and published orbit states (codified as Two-Line Element sets or TLEs) can be compared with TLEs published well after the event in more “refined” orbits. The set of debris fragments can then be constructed once the Space Surveillance Network (SSN) has successfully tracked AND properly associated those fragments with the original event.

The association process is lengthy and imprecise, but typically is performed by trending of specific orbital elements derived from multiple Orbit Determination (OD) test runs over a span of time. A newly tracked object’s orbit inclination coupled with its right ascension of the ascending node can be compared to the long-term nodal evolution (nodal regression rate) as a part of the process. Unreleased analyst satellites can therefore be evaluated to ascertain if they came from the collision.

In this evaluation, we closely examined the orbits of the fragments and their associated location at the time of conjunction as well as the velocity differences with respect to the parent satellite. Our initial assessment found that debris fragments can literally circle the entire globe within a narrow range of orbit planes when back-propagated from their epochs to the intercept event (Time of Closest Approach or TCA) – a situation that’s exacerbated by public TLE releases introducing lengthy delays from the original impact. We relied on the association performed by JSpOC as we did not have access to the original observations, nor analyst satellites with which to perform an independent association evaluation.

We found that adjusting the B* drag term of each debris fragment’s orbit state was able to correct a substantial portion of the satellite positional differences, and thus performed a simple iteration to get the satellites “closer” at the TCA time. We note that further iterations did not yield increasingly accurate results but did expend significant computational resources. This means there is likely another parameter or

two that also needs to be adjusted to fine tune the debris fragment orbital state initial conditions. However, since the results from the B* analysis were generally less than several kilometers, this seemed an adequate first step.

The technique we used evaluated differences in arguments of latitude since we didn't want to change the orbit plane and size unnecessarily. The change on each iteration used the difference in the argument of latitude between the parent and the resulting debris objects, and the initial separation. The resulting spread velocities are depicted in **Figure 3**, with the vector lengths indicating the relative velocity magnitude and the vectors indicating directionality of the imparted spread velocity.

Once the imparted spread velocities have been determined at the intercept time, the spread velocity distribution for tracked fragments can be assessed as shown in **Figure 4**. For this set of debris fragments which were tracked by the SSN, spread velocities can be observed to be below half a kilometer per second.

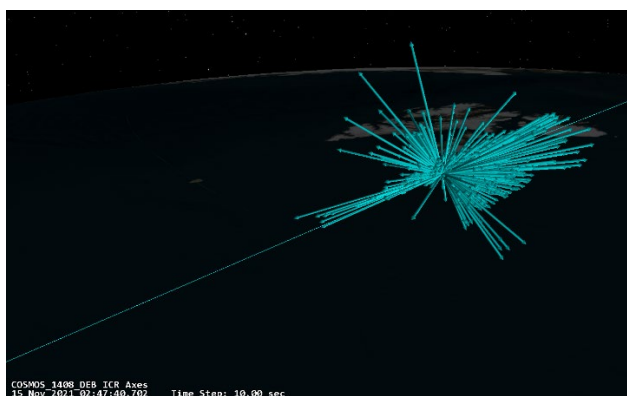


Figure 3: 3D depiction of spread velocities at impact, where vectors denote velocity direction and length denotes relative imparted velocity.

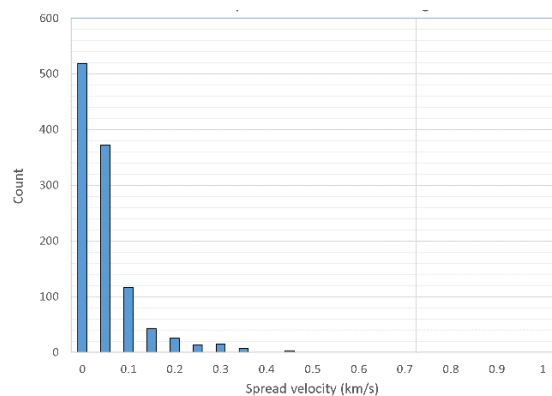


Figure 4: Distribution of relative velocities.

2.4. Assembling the intercept scenario

With an estimated intercept time in hand, the team then found three publicly available Notices to Air Missions (NOTAMs) (**Figure 5**) and orbit and spacecraft data to infer the likely ASAT engagement scenario employed. The selected interceptor trajectory was designed to launch from Plesetsk (NOTAM1) with a flight path angle roughly aligned from Plesetsk toward NOTAM2 and a ballistic reentry designed such that interceptor fragments would generally reenter within the NOTAM3 area. This resulted in an estimated relative velocity between the ASAT interceptor and the COSMOS 1408 target spacecraft in our representative engagement of approximately 4.6 km/s.

2.5. Intercept at the lower limits of hypervelocity

The estimated relative velocity is slightly less than a true “hypervelocity” collision (which is spacecraft material dependent, ranging from 3 to 6 km/s). Unfortunately, most low- to medium-fidelity breakup models are empirical (based on observations and lab test fire statistics) rather than upon theoretical “hydrocode” modeling that can incorporate spacecraft materials, finite element analyses, detailed collision modeling including attitude/orientation, percent overlap, shear angles, involved versus non-

involved structures, plastic deformation, etc. Unfortunately, most of the details required to run a hydrocode breakup model are typically unavailable [7].

The number of tracked COSMOS 1408 debris fragments for which orbit data has been published on space-track is shown in **Figure 6**, with the total number of fragments with publicly released orbit information depicted by the top blue line, and the number of fragments remaining in orbit as of 25 February 2022 shown in the lower red dotted line. As the figure indicates, there are 1,561 debris fragments that have been tracked to date, with under 20% having reentered in the three months that have elapsed since the test.

Because the estimated 4.6 km/s velocity fell just within the 3 to 6 km/s lower limit range for hypervelocity impact, the analysis team selected a fragmentation model [8, 9] that is based upon the NASA Standard Breakup Model [10] (that additionally adheres to first principles and physics conservation laws) and is further enhanced by both ESA MASTER model refinements [11] and low velocity tailored scale factors [12]. It was recognized that this lower velocity may yield fewer fragments than the hypervelocity breakup model may predict, such that the 3,000 trackable fragments initially estimated by our model in its first invocation may be higher than what occurred. The announcement by the U.S. of tracking 1500 fragments during the first day alone (and anticipated detection and orbit custody of many more over the coming months) serves as a lower bound on the number of fragments created.

To account for that, an overall comparison of the actual tracked debris fragments (depicted in orange in **Figure 7**) with the fragments predicted by the selected breakup model (depicted by the white dots in **Figure 7**) was conducted, and the breakup model's configuration was adjusted to best align the model's estimated amount of trackable fragments* with the number of fragments actually tracked as of mid-January 2022. Since that time, the number of tracked fragments has continued to increase, but the rate of increase of tracked fragments now appears to be slowing.



Figure 5: Three Russian “Notice to Air Missions” (NOTAMs) in effect during this test

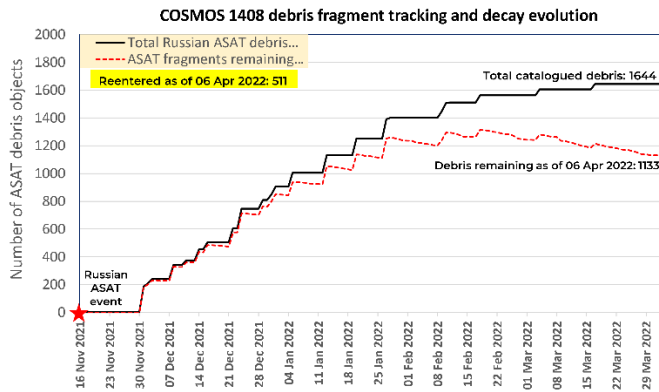


Figure 6: COSMOS 1408 debris fragments tracked to date.

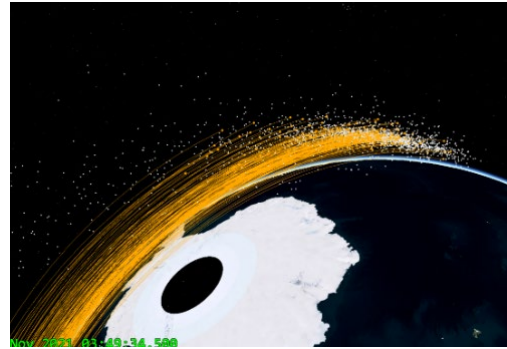


Figure 7: Comparison of actual (tracked) COSMOS 1408 debris cloud vs representative breakup model scenario.

2.6. Modeling ASAT event and space environment impact on operators

With a roughly calibrated intercept and breakup scenario in hand, the overall degradation of the space environment due to the ASAT test can now be assessed. First, a Gabbard plot associated with the discrete breakup model simulation is shown in **Figure 8**. The corresponding orbit lifetime distributions corresponding to both the discrete breakup simulation and actual tracked debris fragments is shown in **Figure 9** and **Figure 10**.

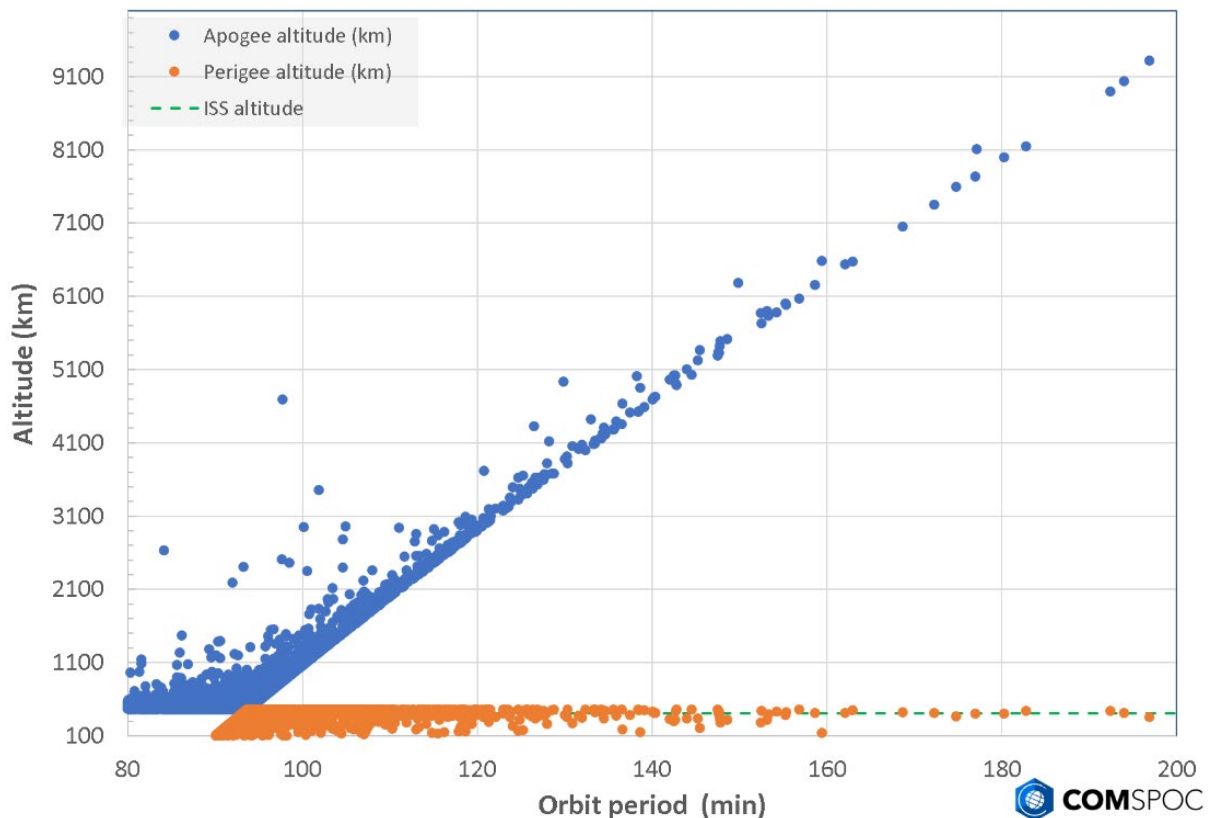


Figure 8: Gabbard plot for all Russian ASAT debris larger than 1cm.

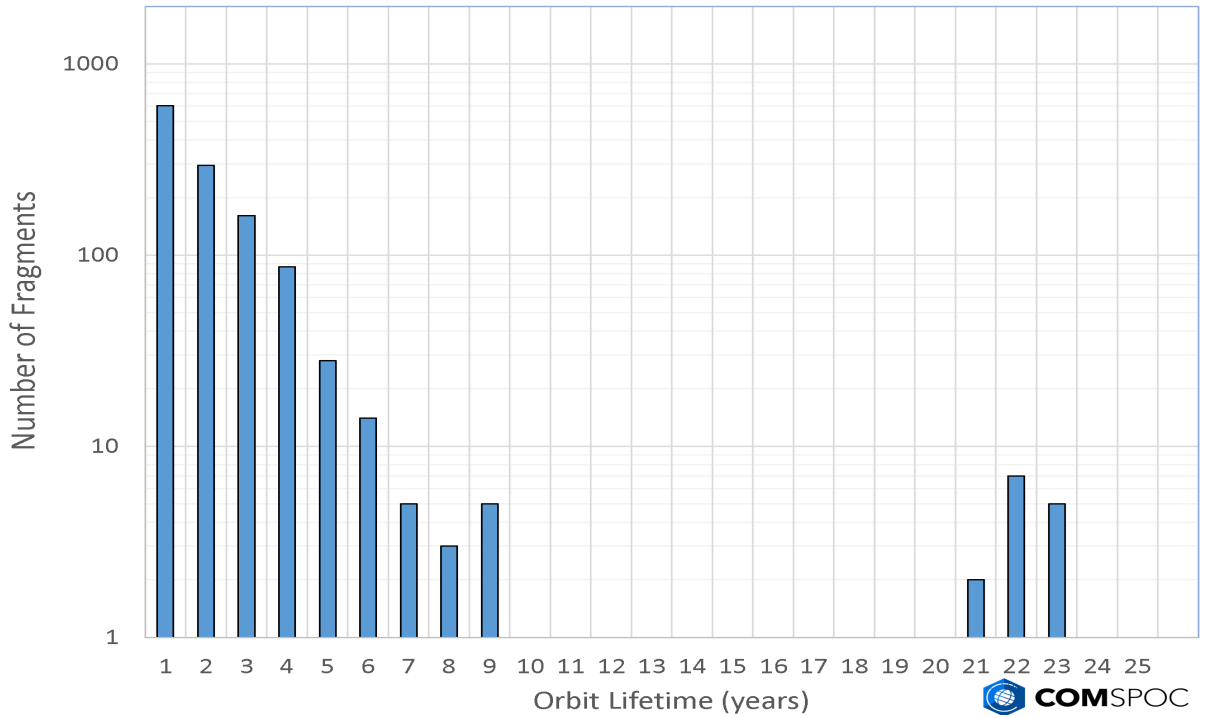


Figure 9: Orbit lifetime distribution for ASAT debris > 5cm (simulation).

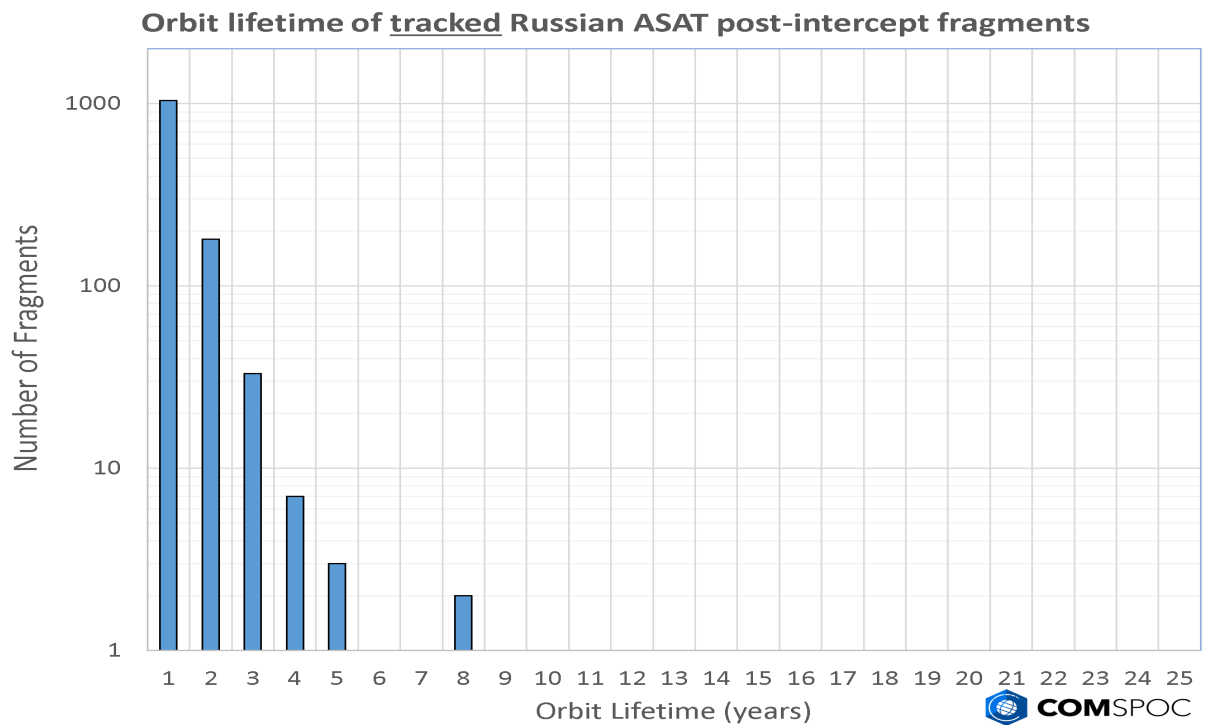


Figure 10: Estimated orbit lifetime distribution for tracked ASAT debris.

2.7. 3D simulation of fragmentation cloud evolution

A 3D simulation following intercept is shown in **Figure 11**. Results from both a discrete (green lines and dots) and a continuum (red volumes) breakup simulation are superimposed. The figure shows ASAT interceptor debris (upper red volume) and COSMOS 1408 debris (lower right red volume) 80 seconds after intercept occurred. The volumetric depiction indicates where fragments could possibly go in a given time of flight, and the color of the volumetric assessment indicates the likelihood that a fragment will actually be present at that location at that time. As time elapses and the volumes start to spread out with no additional fragments being generated, the likelihood of fragments being present decreases, and the red color transitions to yellow as shown in **Figure 12** with the interceptor fragments falling into NOTAM3 and the COSMOS 1408 debris cloud continuing in its overflight of the Aleutian Islands and Hawaii. After a half orbit has elapsed, all debris fragment orbit planes must intersect to make a “pinch line” as shown in **Figure 13**. Within three orbit revolutions (≈ 4.5 hours), the debris volume occupies the entire orbit as shown in **Figure 14**.

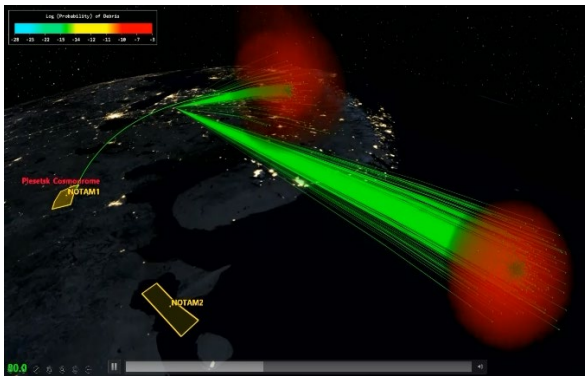


Figure 11: Results of two breakup models (discrete and continuum) overlaid in space as a function of time since intercept.

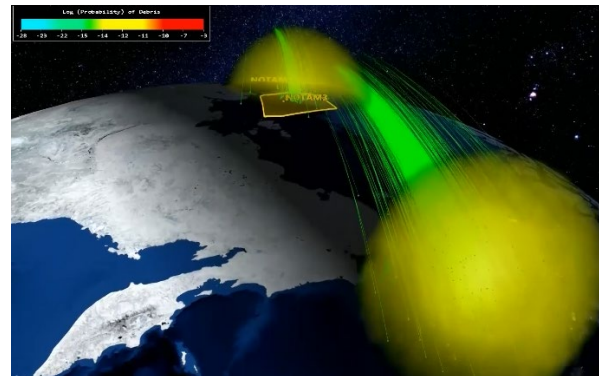


Figure 12: Interceptor debris reentering into NOTAM3 area with COSMOS 1408 debris volume continuing to expand.

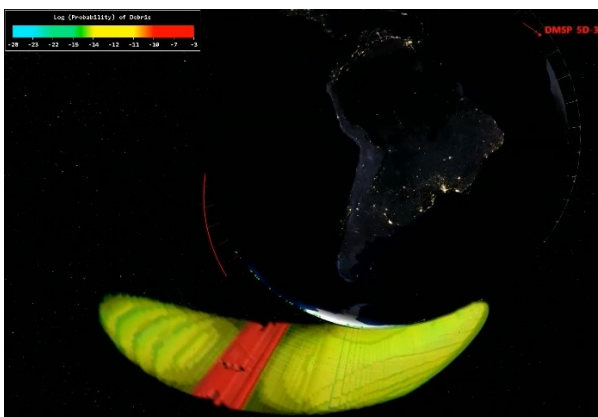


Figure 13: Likelihood of a fragment's presence is heightened at the “pinch line” where debris fragment orbit planes intersect, 180° away from the intercept location.

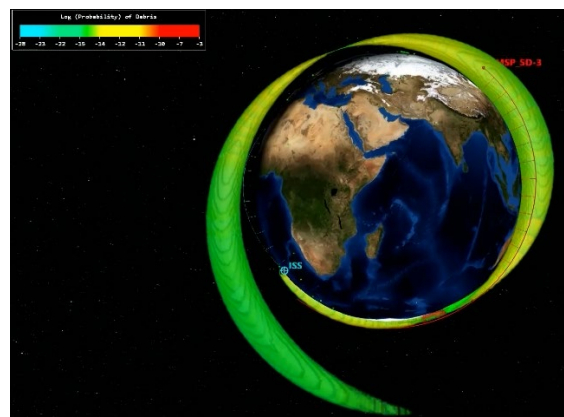


Figure 14: COSMOS 1408 debris volume occupies the entire orbit within only three revolutions.

2.8. Modeling ASAT event and space environment impact on operators

The volumetric characterization is useful in several ways: (1) It helps convey understanding of how the debris cloud evolves with time; (2) it allows the analyst to discover where, in aggregate, the debris could go and the likelihood of it being present there over a timespan of interest (for example, the first 24 hours as shown in **Figure 15**), and (3) it allows the analyst to “fly all active spacecraft through the debris volume” to determine the integrated relative risk to spacecraft as summarized in **Figure 16**.

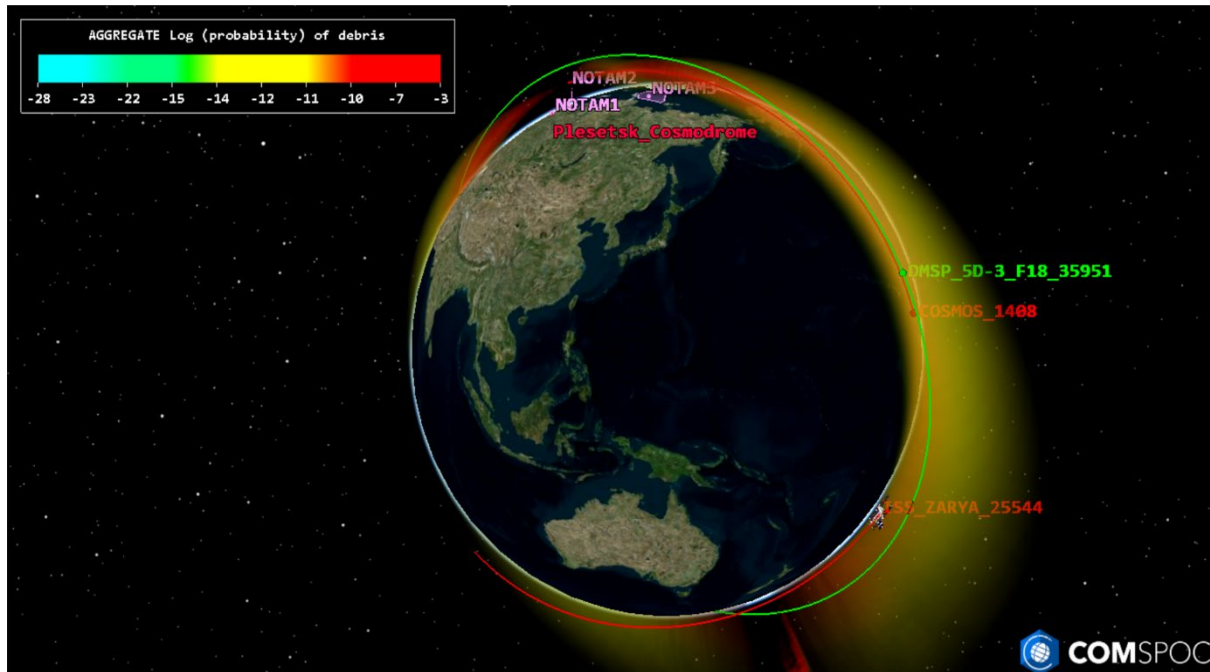


Figure 15: Aggregate volume debris fragments occupy during first 24 hours after intercept, coloured by likelihood of a fragment’s presence.

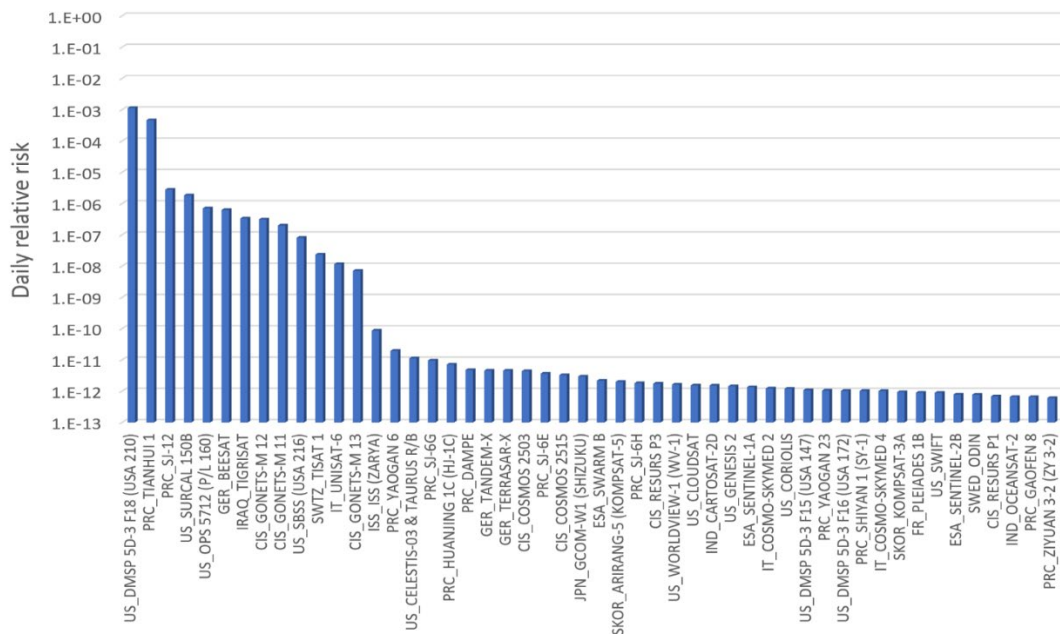


Figure 16: Top 50 at-risk satellites in first 24 hours.

It is instructive to examine why these satellites were placed at greatest risk. As seen in **Figure 17**, there are two conditions which caused active spacecraft to be at heightened risk: (1) the active spacecraft was roughly coplanar with the debris volume, or (2) it was not coplanar, but it intersected the volume at locations where debris fragments were most likely to be present.

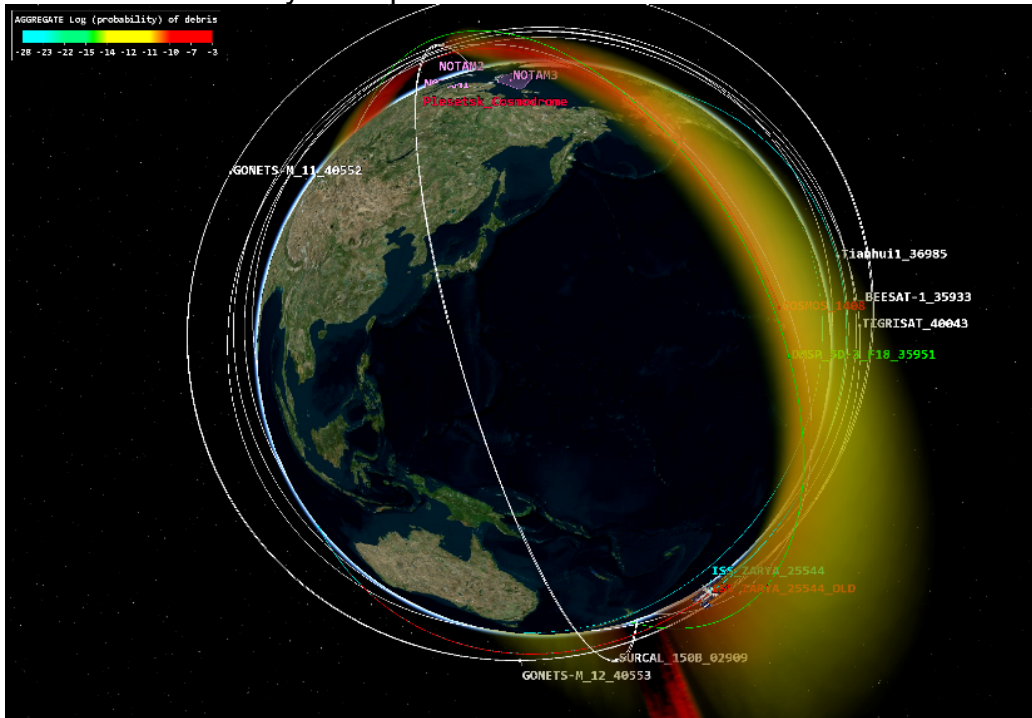


Figure 17: Orbits of Top 50 at-risk satellites relative to the debris volume.

The at-risk spacecraft can also be examined as a function of time to determine precisely when they are placed at greatest risk, as shown in **Figure 18**.

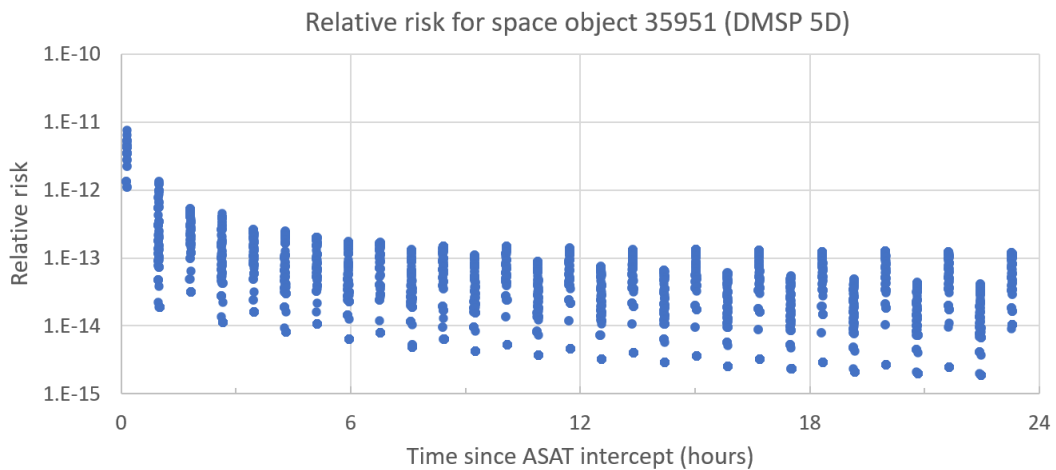


Figure 18: Twice-per-revolution collision risk cycle for DMSP 5F-3 F18.

3. Comparison of Russian ASAT event with other significant breakups

It is helpful to compare this fragmentation event with other ASAT events as shown in **Table 1**, where the dates, altitudes, relative velocities, catastrophic breakup metrics, and debris quantities and lifetimes are compared. The rows contain the following comparative information:

- In row 4, the relative velocity has been estimated to determine if the intercept's relative velocity exceeds the speed of sound in the material the spacecraft is constructed from (for example, steel ranges from 3.1 and 6 km/s and aluminum from 3.8 to 6.5 km/s).
- Row 5 contains the estimated energy per unit mass, which is assessed to determine if the collision can be considered as a catastrophic collision (with greater than 40 Joules per gram being considered as a rough guide) - - and all events can be seen to be catastrophic as they greatly exceed this criterion.
- Row 6 contains the number of fragments that have been tracked by the Space Surveillance Network at some point following the breakup. Rows 7 and 8 contain our simulated breakup results by comparison, where a "trackable" object is assumed to be larger than 5 cm in size with an orbit lifetime exceeding one day, and Lethal Non-Trackable objects (LNTs) are assumed to be smaller than 5 cm and larger than 1 cm.
- Row 9 contains the 80th-percentile orbit lifetime, meaning that 80% of all fragments will have reentered before this time.
- Rows 10 and 11 serve as a proxy for overall adverse effect on the environment by summing up the estimated orbit lifetimes for all trackable and LNT objects, respectively.

While the Iridium/Cosmos breakup was an accidental collision and not an ASAT test, it is understandable to ask how these ASAT tests compare with that collision event as shown in **Table 2**.

Taken together, these tables indicate that the Chinese ASAT test was by far the most harmful to the environment, with the Russian ASAT test ranking second in terms of harmful ASAT tests. The Iridium/COSMOS collision was quite harmful as well, but not as much as the Chinese ASAT test.

Figure 19 summarizes these and other breakup events from the start of the space program to present. The gray vertical bars denote the number of debris fragments tracked by the Space Surveillance Network at some point, while the red vertical bars signify the number of fragments still on orbit as of 1 January 2022.

4. Increased spacecraft operator workload

Figure 20 reveals average, annual, encounter rates in 25 km altitude bins that the global LEO active spacecraft population is likely to experience in January 2022. The bar chart was created using the "Probability and Frequency of Orbital Encounters" tool (U.S. Patent No 10293959) whose inner workings are explained in the paper "Volumetric Assessment of Satellite Encounter Rates." [13]. We separated the <https://space-track.org>, January 14, 2022, TLE catalog into active and inactive satellites. The inactive satellites were then further separated into COSMOS 1408 ASAT trackable debris and all other inactive objects, thereby representing the RSO debris prior to intercept. Three separate encounter categories were then considered:

active-on-active (blue bars), active-on-RSO debris (orange bars), and active-on-COSMOS 1408 ASAT debris (gray bars). For the active-on-active analysis, we assumed no fratricidal encounters with respect to the same owners/operators (i.e. we excluded consideration of Starlink-v-Starlink, Iridium-v-Iridium, etc.). We also assumed no remediation or attempt at avoidance.

The combination of blue and orange bars shows the encounter rate prior to the Russian ASAT test. The gray bars show the additional encounter burden placed on the space community. As the ASAT debris decays, the gray bars will decrease in altitude, eventually passing through ISS altitude.

Table 1. Comparison of Russian ASAT event with other ASAT breakups.

Category	Chinese ASAT	USA 193	Indian ASAT	Russian ASAT
Date	11 Jan 2007	21 Feb 2008	27 Mar 2019	15 Nov 2021
Altitude (km)	856	246	282	461
Velocity (hypervelocity $\sim > \approx 6$)	14.8 km/s	8.49 km/s	9.4 km/s	4.6 km/s
\approx kJ/kg (catastrophic $\approx >40$)	15,000-35,000	1,500 - 2,500	6,000	500 - 1,000
Debris tracked by SSN	3,532	174	129	1,510 (so far)
Simulated trackable* debris	3,007	452	936	1,246
Simulated Lethal Non-Track	34,733	3728	10,439	16,386
80 th percentile lifetime (yrs)	63	0.03	0.05	1.5
“RSO-years” (trackable)	130,347	13	65	2,098
“RSO-years” (LNT)	1,225,972	94	784	16,464

Table 2. Estimated effect of Iridium/Cosmos collision.

Iridium/Cosmos collision
10 Feb 2009
769
11.6 km/s
51,500
2,369
2,651
7,883
56
108,230
257,442

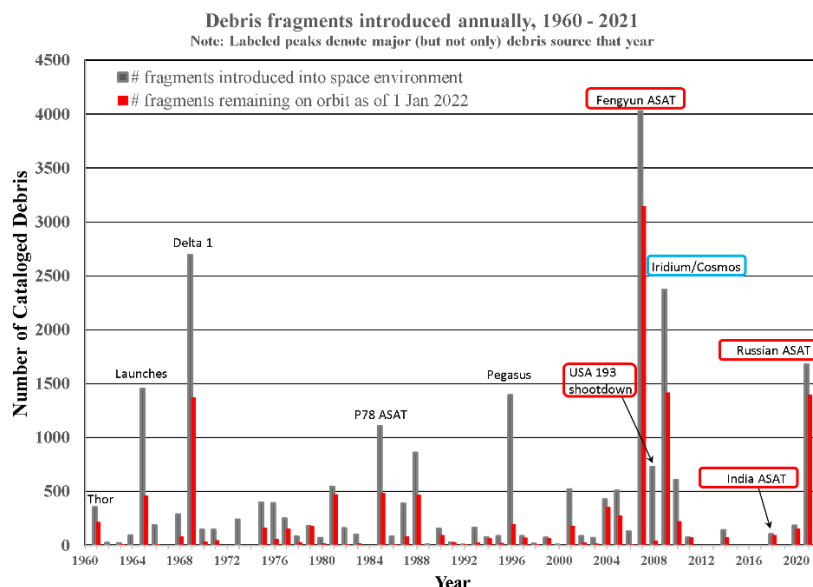


Figure 19: COSMOS 1408 debris volume occupies the entire orbit within only three revolutions.

5. Heightened conjunction rates and collision risk for Sun-synchronous orbits

In the wake of the Russian ASAT test, one aspect that was not immediately apparent was the dramatic spike in number of conjunctions, collision risk, computational burdens, and risk management that the COSMOS 1408 debris field subjected the spacecraft operator community to for spacecraft in Sun-synchronous orbits or for large constellations. In this section, we'll examine why the conditions were extremely unfavorable for typical Earth observing systems, how that translated into heavy workloads for both government and commercial Space Situational Awareness (SSA) conjunction detection and notification systems, how the collision risk is projected to as much as double, and implications on automated collision avoidance maneuvering systems and maneuver frequencies.

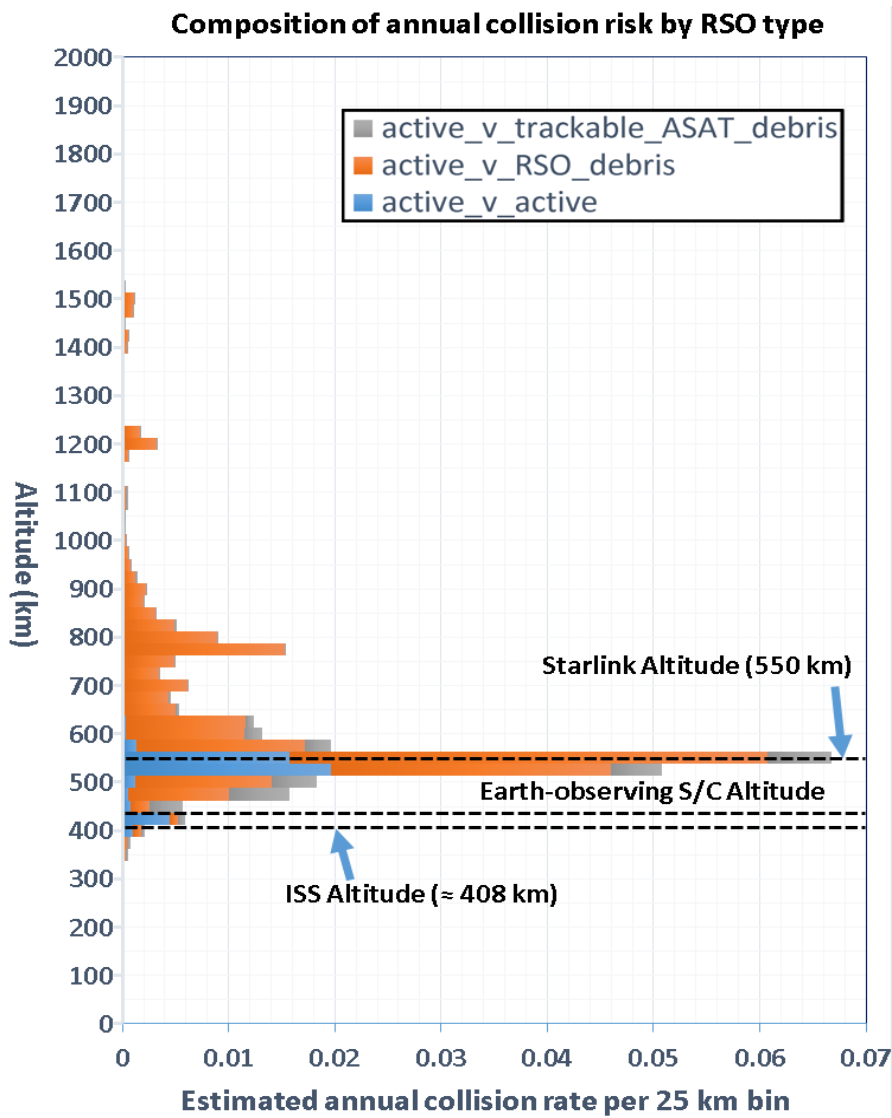


Figure 20: Breakdown of collision risk for active-vs-non-COSMOS 1408 debris (orange), active-vs-active (blue) and active-vs-COSMOS 1408 debris.

5.1. Planet's mission, spacecraft constellations, and orbits

Planet operates the largest fleet of Earth observation (EO) satellites to date. The operational fleet consists of over 150 medium resolution Dove satellites and 21 high resolution SkySat satellites (**Figure 21**). For the purposes of this section of the paper, we focus on the Dove fleet.



Figure 21: Planet's fleet includes Doves (left) and SkySats (right).

In the aftermath of the Russian ASAT test on COSMOS 1408, the major effects to Planet's operations were:

- Increased Conjunction Data Message (CDM) volume caused internal conjunction assessment run-times increased by up to 66% during the December/January conjunction squall.
- Increased CDM volume caused internal conjunction assessment failures from exhausting system memory
- Increased CDM volume that caused Space-Track alerts for exceeding API usage quotas.
- Revised training for Planet's on-call operators for managing conjunctions, resulting in an increased workload for operators.

Despite the dire situation, to-date, Planet has not had to make an avoidance maneuver for a COSMOS 1408 debris object.

Dove satellites are 3U CubeSats that nominally operate at altitudes of 350 km to 525 km, i.e., in band with the COSMOS 1408 debris cloud (**Figure 8**). The high-level orbital parameters of interest for Planet's Dove fleet are provided in **Table 3**.

The internal volume is mostly occupied by the imaging payload. As such, Doves do not have room for a propulsion system for performing orbital maneuvers. They are reliant on differential-drag maneuvers for phasing and station-keeping [14].

Due to the large size of Planet's fleet, an automated collision avoidance pipeline has been developed as shown in **Figure 22** to alert and act on close approaches.

Planet's automated collision avoidance pipeline is designed to act on conjunction screenings provided by external services. The pipeline will automatically schedule an avoidance Diff-Drag maneuver for conjunctions with $P_c > 1e-4$ for and $TCA < 72$ hours. LeoLabs has previously demonstrated, in a collaboration with Planet, that Diff-Drag is an effective method of reducing the collision risk during conjunctions [15]. Space-Track and Space Data Center (SDC) are the primary screening

providers, although the system is designed so that additional services can be easily added.

Table 3. Orbital parameters of interest for Planet’s Dove fleet.

Flock	Inc [deg]	MLTDN	Mean SMA Altitude [km]
Flock 2k	96.82	19:30	368
Flock 3k	96.82	22:15	464
Flock 2p	97.25	9:37	459
Flock 3p	97.30	10:06	461
Flock 3p’	97.40	10:49	482
Flock 3m	97.43	12:50	481
Flock 4a	97.33	9:33	479
Flock 4p	97.42	9:49	490
Flock 4e’	97.44	9:44	505
Flock 4v	97.44	10:17	518
Flock 4s	97.46	9:30	521
Flock 4x	97.50	10:00	524

The pipeline analyzes the latest CDMs every 2 hours. This ensures that the latest state vectors for Planet’s satellites can be used to reassess. Planet uses the Alfano 2005 technique for computing miss distance and P_c . The increased CDM volume from conjunction squalls has necessitated refactoring of the conjunction assessment system. Memory usage has been decreased by loading fewer CDMs into memory at a time during Planet Conjunction Assessment. Run-time has been decreased by horizontally scaling the Planet Conjunction Assessment across containerized instances that run for a single satellite. These updates will be evaluated during the April 2022 squall we will depict in **Figure 32**.

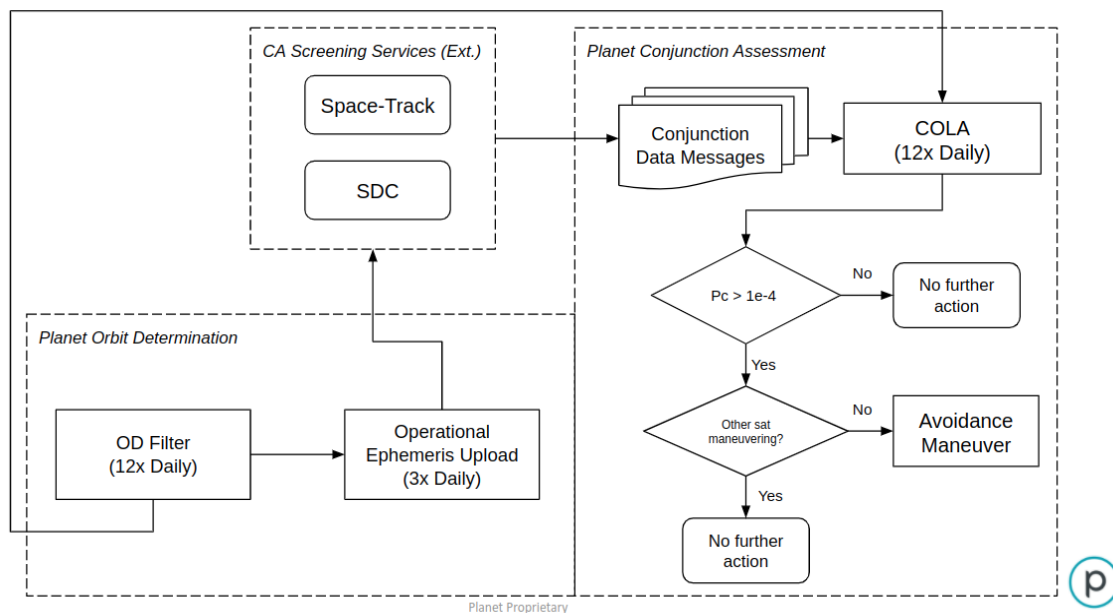


Figure 22: Planet automated conjunction avoidance pipeline.

The Russian ASAT test and its resultant debris cloud have been of concern for Planet since it was first reported. It is likely that there have been more high-risk close approach scenarios between Planet assets and COSMOS 1408 debris than the CDM counts indicated. This is because it takes a significant amount of time for SSA providers, such as 18SPCS, to catalog the debris from these types of events, and as a result, satellite operators were effectively flying blind for many weeks after the event. Planet spent personnel time in an attempt to model COSMOS 1408 debris clouds directly after the ASAT test, but the work did not produce actionable results. Analytical methods can produce high level estimates for collision risk and number of close approaches. However, with the current state of technology, operators require screenings against individually cataloged objects in order to determine a course of action.

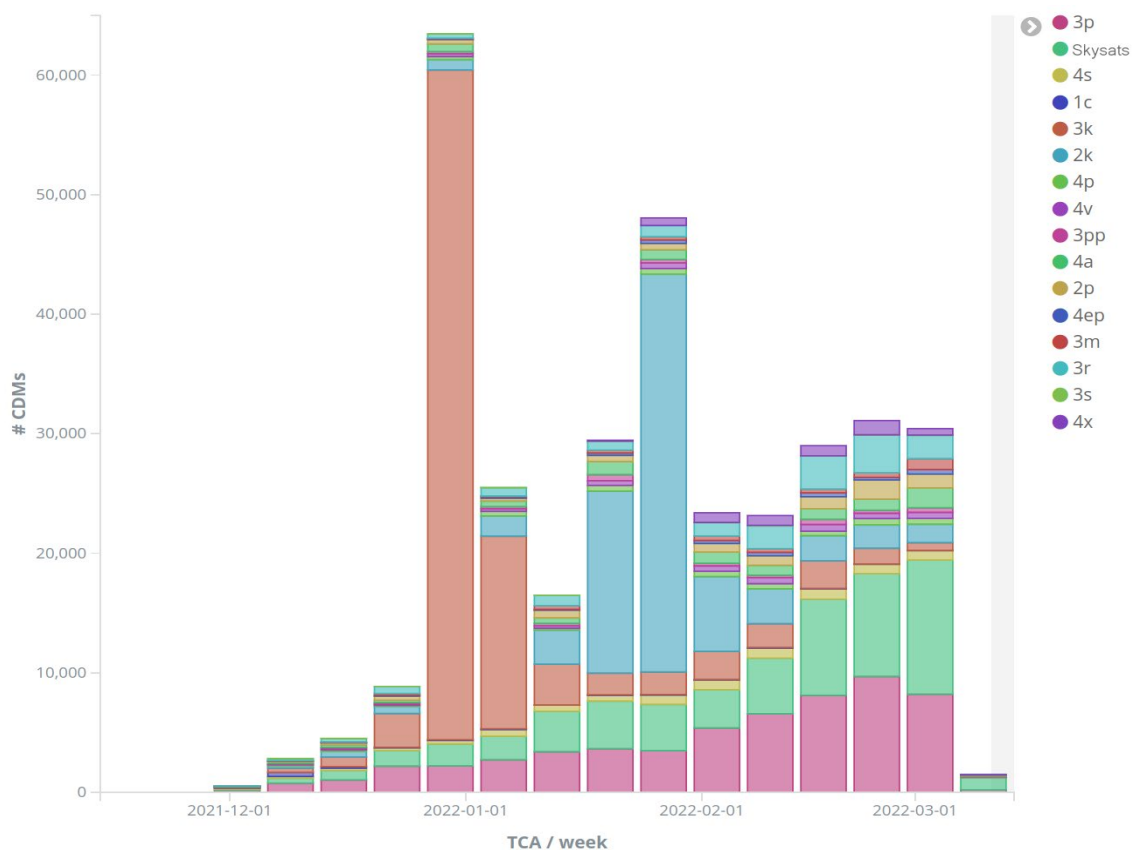


Figure 23: Weekly number of CDMs generated by 18SPCS for close approaches between Planet satellites and COSMOS 1408 debris.

Planet observed the first conjunction squall from the COSMOS 1408 debris on the week of 2021-12-27. During that time period, over 60,000 Conjunction Data Messages (CDM) were generated for Planet satellites by 18SPCS.

Of the over 60,000 CDMs during this squall, 56,000 of them were for Flock 3k satellites (**Figure 23**). At that time, it was unclear if this indicated a new exceptional risk for that particular orbit plane; fortunately, this was not the case. During these

time periods satellite operators were put on high alert to monitor for high risk CDMs with COSMOS 1408 debris. Planet expects the CDM volume to increase as more debris gets cataloged.

5.2. Space Data Center detection of “Conjunction Squalls”

The Space Data Center has been fully operational since 2010, providing flight safety services to over 30 operators occupying all earth-orbiting regimes (LEO, Middle Earth Orbit or MEO, and Geosynchronous Earth Orbit or GEO).

On 2 January 2022, a twenty-fold increase in the number of daily conjunctions was observed for Planet’s 168 FLOCK spacecraft as seen in **Figure 24**. Such a spike, which we refer to as a “**conjunction squall**,” a localized furiosity of conjunctions in a short period of time, can adversely affect conjunction runtimes, flight safety notification bandwidth, and spacecraft safety.

The SDC Operations team and Center for Space Standards and Innovation (CSSI) personnel immediately investigated to determine why this had occurred.

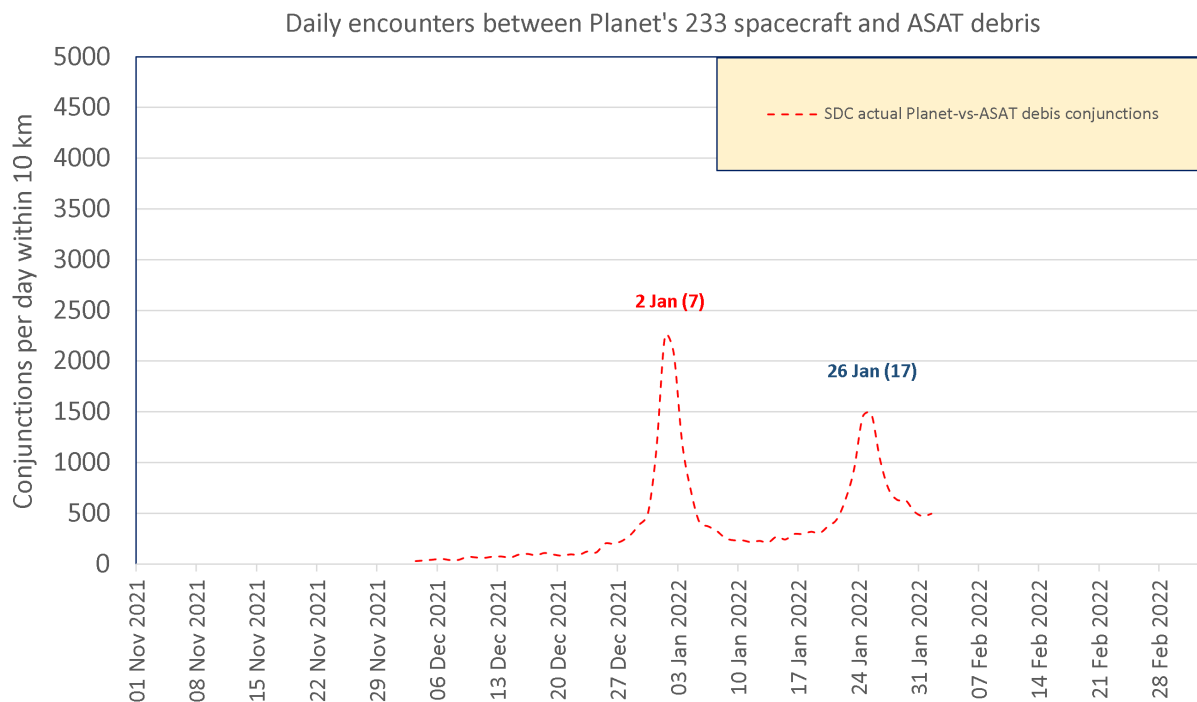


Figure 24: Factor of 20X spike in FLOCK conjunctions with ASAT debris.

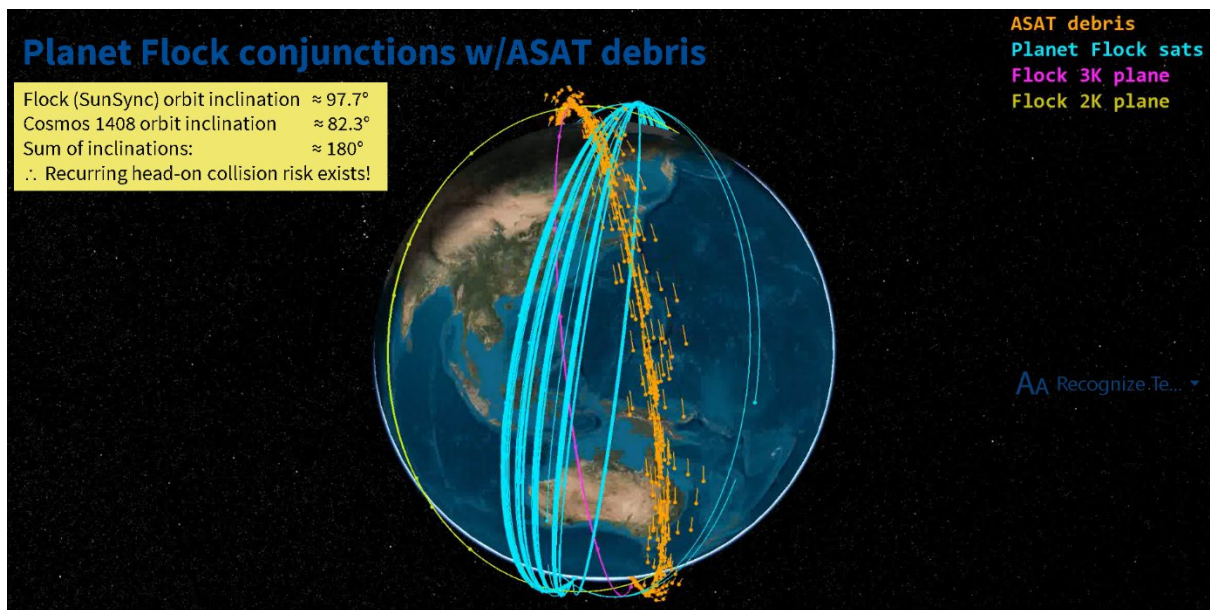


Figure 25: Planar orientation of COSMOS 1408 debris (orange) and Planet constellations on 25 December 2021.

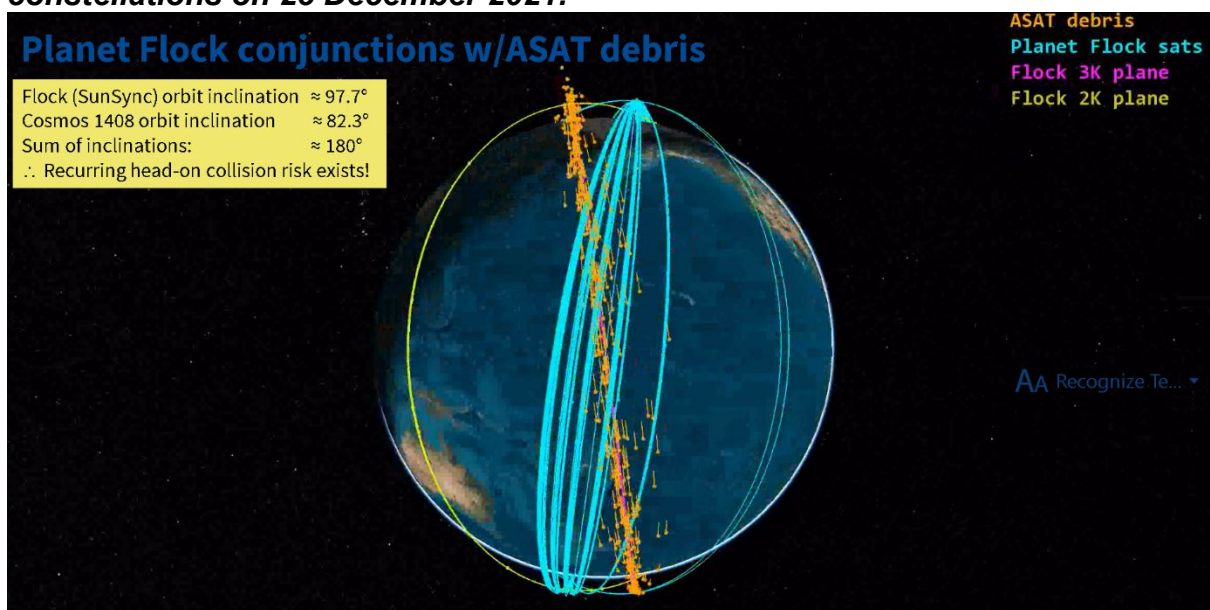


Figure 26: Planar orientation of COSMOS 1408 debris and Planet constellations on 2 January 2022, with COSMOS 1408 debris coplanar and counter-rotating against Planet FLOCK spacecraft.

A visualization of the orbit planes told the story: **Figure 25** shows the planar orientation of both debris and Planet spacecraft at a relatively quiescent period (25 December 2021), whereas **Figure 26** illustrates how on 2 January 2022 the orbital debris occupied the same orbit plane as the Flock 3K satellites. Working closely with Planet, the team quickly identified the underlying cause. The COSMOS 1408 debris was inclined at roughly 82.3° causing its orbit plane to “regress” (i.e., the orange debris fragments move to the left). Meanwhile, satellites occupying Sun-synchronous orbits inclined at 97.7° would be “progressing” (moving to the right to

match the Earth's rotation rate about the Sun to keep the spacecraft's local time of descending node constant - - typically a requirement for earth observing spacecraft). Because these inclinations add up to 180°, this means not only that twice per year the COSMOS 1408 debris will be coplanar with Sun-synchronous orbits, but it will also be counter-rotating (i.e., head-on collision potential). As a result, conjunctions will be greatly amplified from the normal background situation, with two potential collision threats existing per orbit.

This is not the first time that such conjunction squalls have been observed [16], where the author observed conjunction spikes associated with the Iridium 33/COSMOS 2251 collision debris fragment populations. But notably, the author did not highlight the orbital inclinations of the COSMOS 2251 debris fragments (centered around 74.04°) and Iridium 33 fragments (86.38°) as compared to the WorldView-2 spacecraft's 98.49°. From that perspective, the Russian ASAT intercept of COSMOS 1408 is quite different in terms of introducing the possibility of coplanar, counter-rotating active spacecraft and debris fragments.

5.3. Characterization of COSMOS 1408 debris and Planet spacecraft

At this point, it was clear that we needed to fully characterize the nodal evolution for both Planet spacecraft and COSMOS 1408 debris as shown in **Figure 27**. The figure shows the RAAN values for the various FLOCK spacecraft planes as diagonal lines moving from the bottom left to upper right with a one-year cycle. Each orbital plane is indicated by its color in the legend. The COSMOS 1408's descending nodal progression is indicated by the red and brown lines moving from center left down and to the right. Orbits are coplanar when the COSMOS 1408 descending node is at the same orientation in inertial space as the ascending node of the Planet (or any other Sun-synchronous) orbit. Note that for simplicity, only three pieces of COSMOS debris are represented here.

Colored annotations show crossing date & (# sats affected)

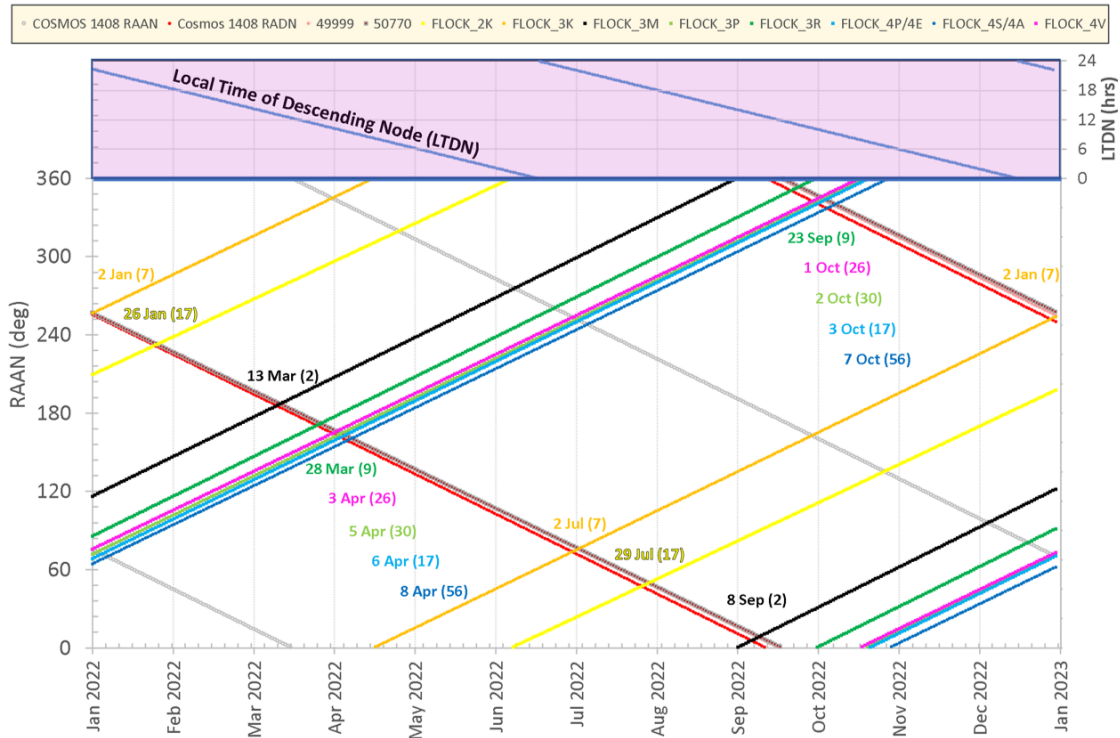


Figure 27: Nodal evolution for Planet FLOCK spacecraft and ASAT debris.

5.4. Determination of Sun-synchronous orbit LTDN during conjunction spikes

The top of **Figure 27** shows the Local Time of Descending Node (LTDN) for a Sun-synchronous orbit were it to be coplanar with the COSMOS 1408 debris orbit plane. LTDN can be readily determined from simplified relationships extracted from the orbit plane geometry shown in **Figure 28**:

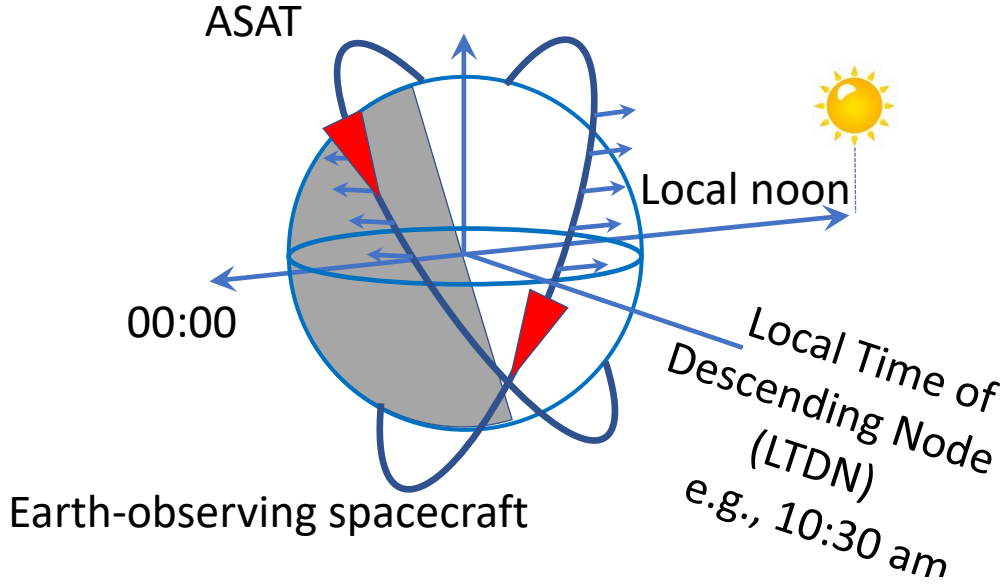


Figure 28: Depiction of geometries from which LTDN can be determined.

$$\text{The right ascension of the Sun } \alpha_s \approx (\text{DayOfYear} - 80 \text{ days}) \left(\frac{360^\circ}{365 \text{ days}} \right) \quad [1]$$

$$\text{Local midnight is located at } \alpha_{\text{midnight}} = \alpha_s + 180^\circ \quad [2]$$

$$\text{The active spacecraft's } LTDN_{S/C} \approx \frac{(\Omega_{S/C} + 180^\circ) - (\alpha_s + 180^\circ)}{15} = \frac{\Omega_{S/C} - \alpha_s}{15} \quad [3]$$

$$\text{COSMOS 1408 debris plane: } \Omega_{1408} \approx 77^\circ - \text{DayOfYear} \quad [4]$$

$$\text{Debris coplanar w/active S/C and counter-rotating when } \Omega_{1408} = \Omega_{S/C} - 180^\circ \quad [5]$$

Combining the above expressions yields:

$$LTDN_{S/C} \approx \frac{\Omega_{1408} - \alpha_s}{15} + 12 \approx \frac{77^\circ - \text{DayOfYear} - (\text{DayOfYear} - 80) \left(\frac{360}{365} \right)}{15} + 12 \quad [6]$$

$$\text{Reducing yields } LTDN_{S/C} \approx 22.39 - 0.1324 (\text{DayOfYear}) \quad [7]$$

The annotations in **Figure 29** indicate that the heavily populated Sun-synchronous Planet satellites conjuncting in early April correspond to mid-morning ($\approx 10\text{am}$) orbit planes.

Colored annotations show crossing date & (# sats affected)

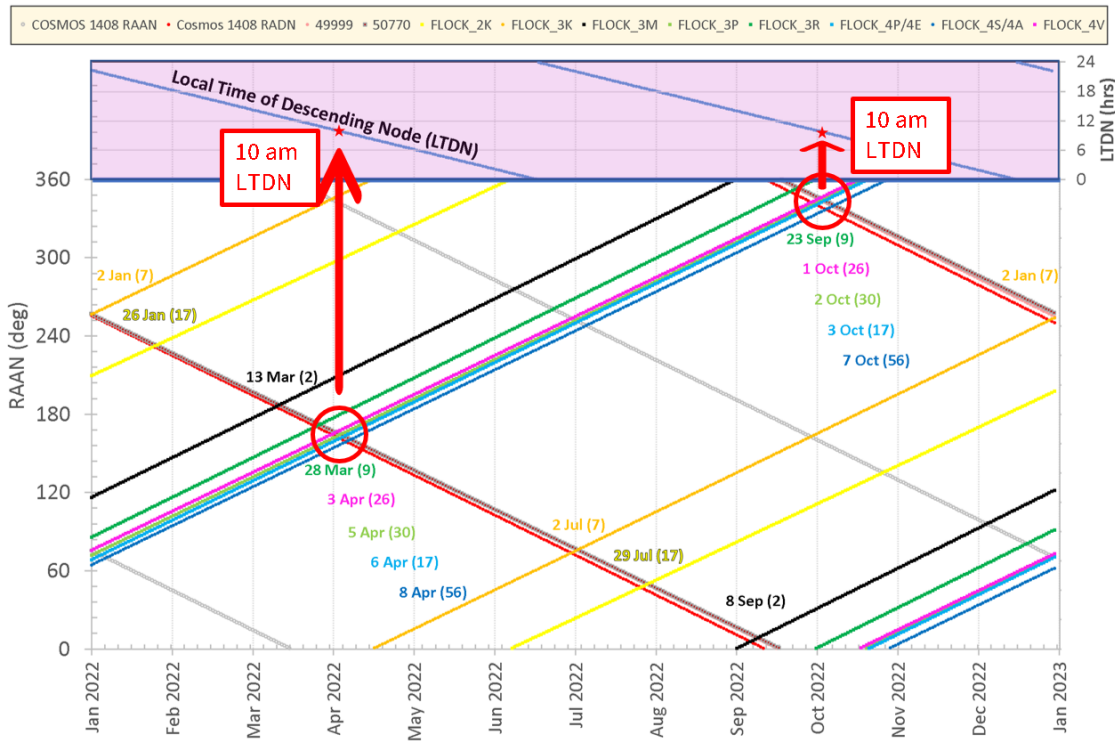


Figure 29: Local Time of Descending Node at coplanar transits.

5.5. Modeling of Conjunction Squalls using volumetric encounter method

As the Space Surveillance Network continued to detect and track new COSMOS 1408 debris, the SDC’s knowledge of the debris fragments and potential collisions of them with the SDC’s active satellites increased and additional conjunctions were identified. Had the SDC been aware in December 2021 of the 1,400 COSMOS debris fragments that Space-Track eventually published as of 29 January, the SDC would have identified even more conjunctions. To account for this effect, the SDC’s number of conjunctions was increased by a simple ratio of the 1,400 fragments as of 31 Jan 2022 divided by the number of fragments the SDC knew about at the time it performed the conjunction analyses. The scaled trend is shown in **Figure 30**.

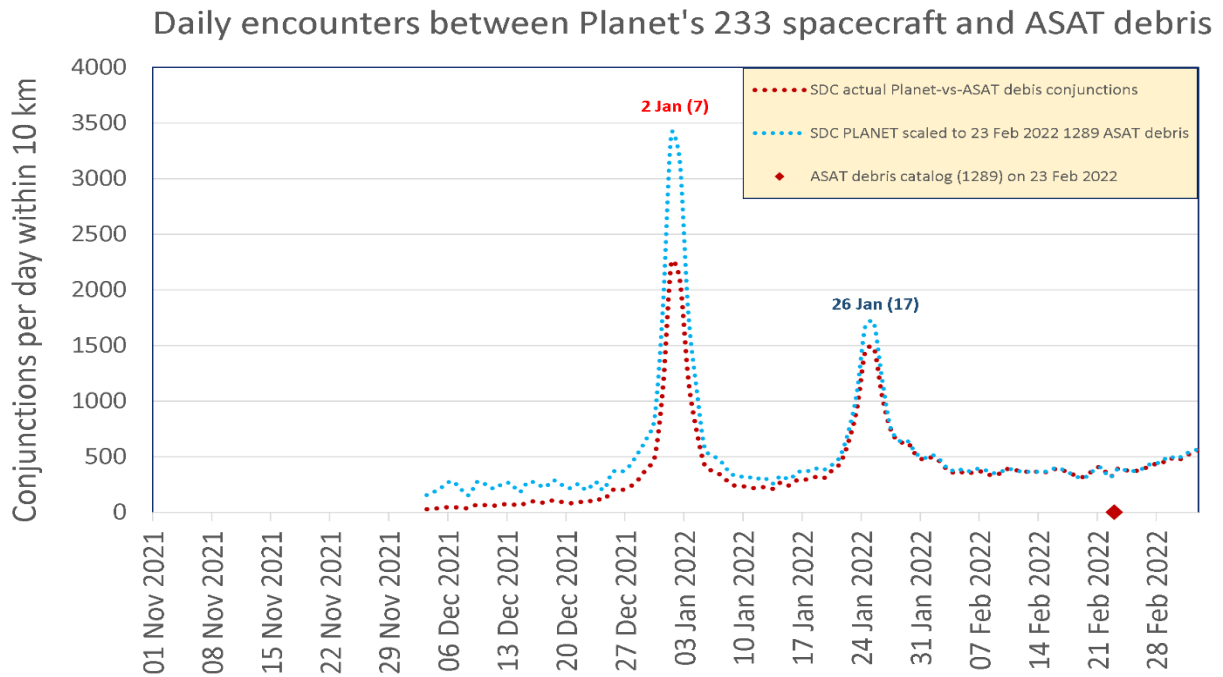


Figure 30: SDC encounters for Planet’s 233 spacecraft scaled by catalog size.

The volumetric encounter rate tool is designed to determine average encounter rates from orbital data. The tool was enhanced to propagate orbital data using SGP4 and then reassess those rates on a daily, changing basis as the predicted orbital elements evolve.

NOTE on exclusion zone shape and size: For these and many of the analyses in this paper, we adopted (for consistency) a 10-kilometer radius exclusion volume as the definition of an encounter, matching the 10 km radius used for some of our larger volume screenings conducted in the SDC. As you will see later, the only exception to this 10 km radius spherical exclusion volume is the so-called “pizza box” we applied to the ISS.

The excellent agreement between the scaled SDC encounter rates (blue dotted line) and those predicted by the volumetric encounter rate tool (black line) and spot checks using STK’s AdvCAT module can be seen in **Figure 31**.

We examined these changing rates by comparing the volumetric encounter rate results to independent computations by System Tool Kit’s AdvCAT module for the same 10km screening distance. As **Figure 31** reveals, this is not an exact comparison. AdvCAT will determine the precise number of encounters over a fixed timespan (e.g., a day), whereas the volumetric tool uses an instantaneous snapshot of orbital elements to determine the number of encounters typically expected to occur at that instant of time. So, while AdvCAT identifies actual, discrete conjunctions, the volumetric encounter tool identifies the typical instantaneous rates. This means that the AdvCAT binned-by-day results will not have the extremes that are (properly) identified by the volumetric encounter algorithm, but the small sample size of the discrete conjunctions will introduce additional variability about the continuous volumetric encounter rate trend.

Estimates of encounter rates can be extended for long periods of time. **Figure 32** and **Figure 33** show our projections for the entire year 2022 using a 23 February

and a 1 April space catalog, respectively. Note the excellent comparison agreement of the Volumetric Encounter Method (VEM) with spot checks using operationally verified tools such as STK Advanced CAT (purple dots).

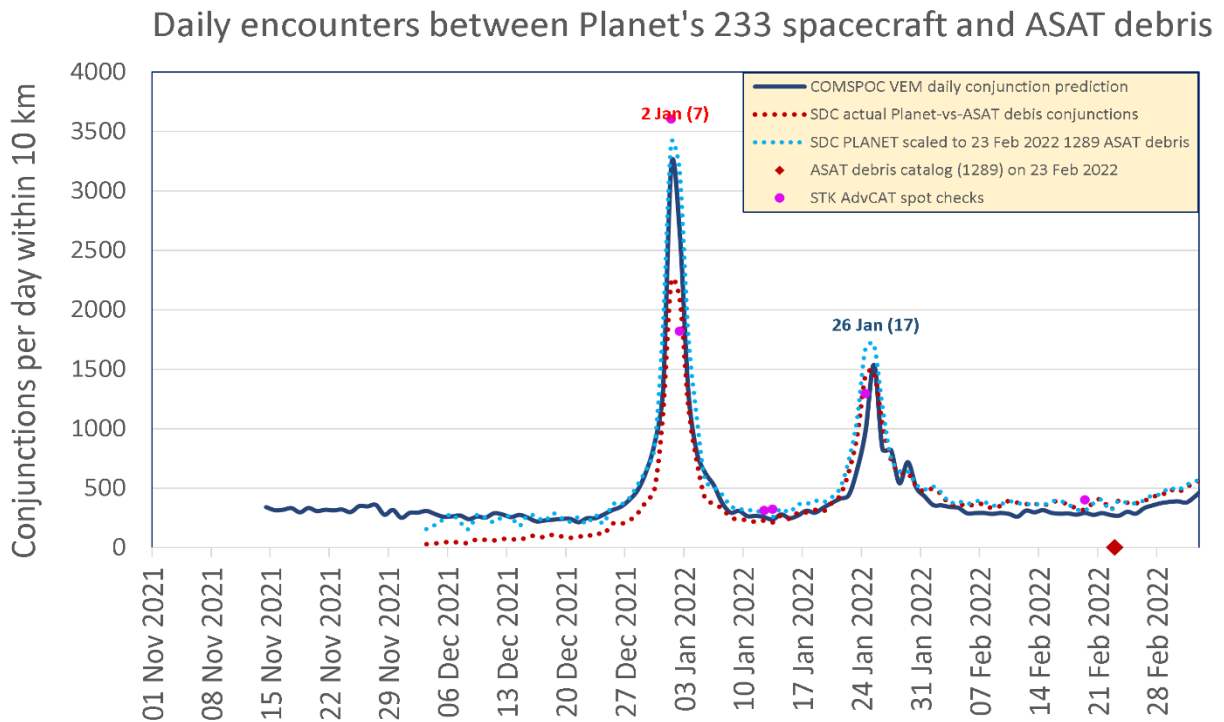


Figure 31: Comparison of volumetric encounter rate tool with SDC and AdvCAT.

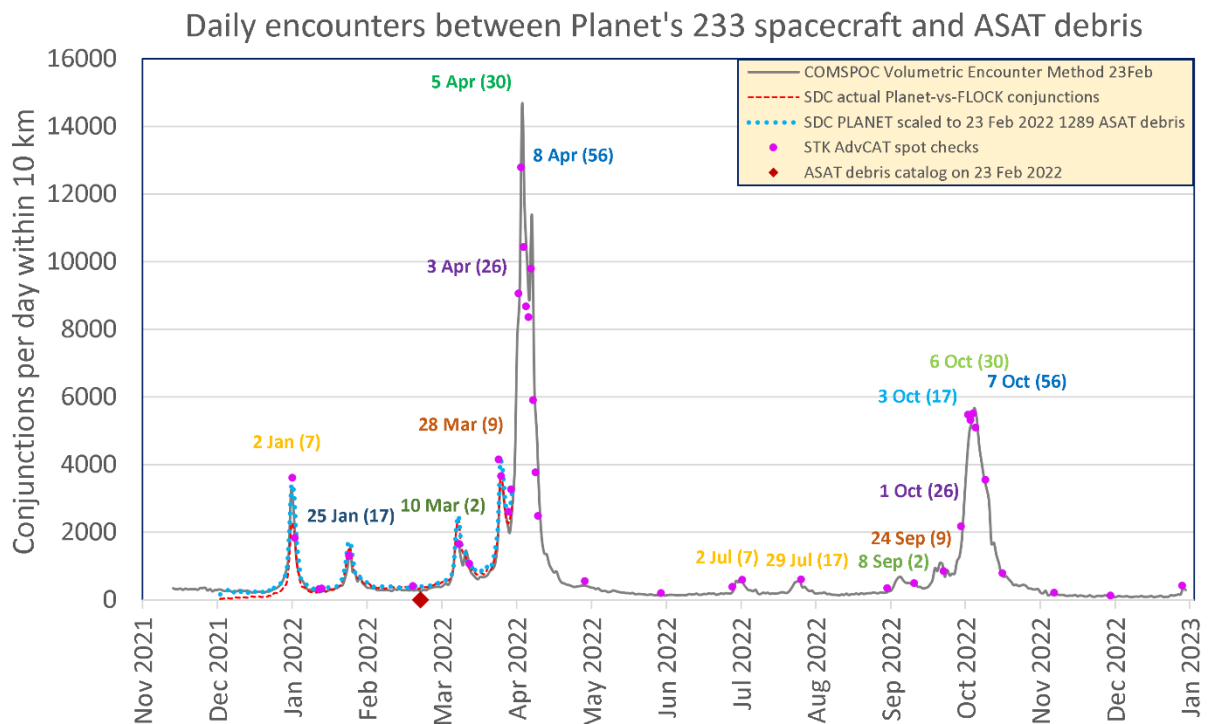


Figure 32: 23 Feb prediction of Planet conjunction rates to end of 2022.

Daily encounters between Planet's 233 spacecraft and ASAT debris

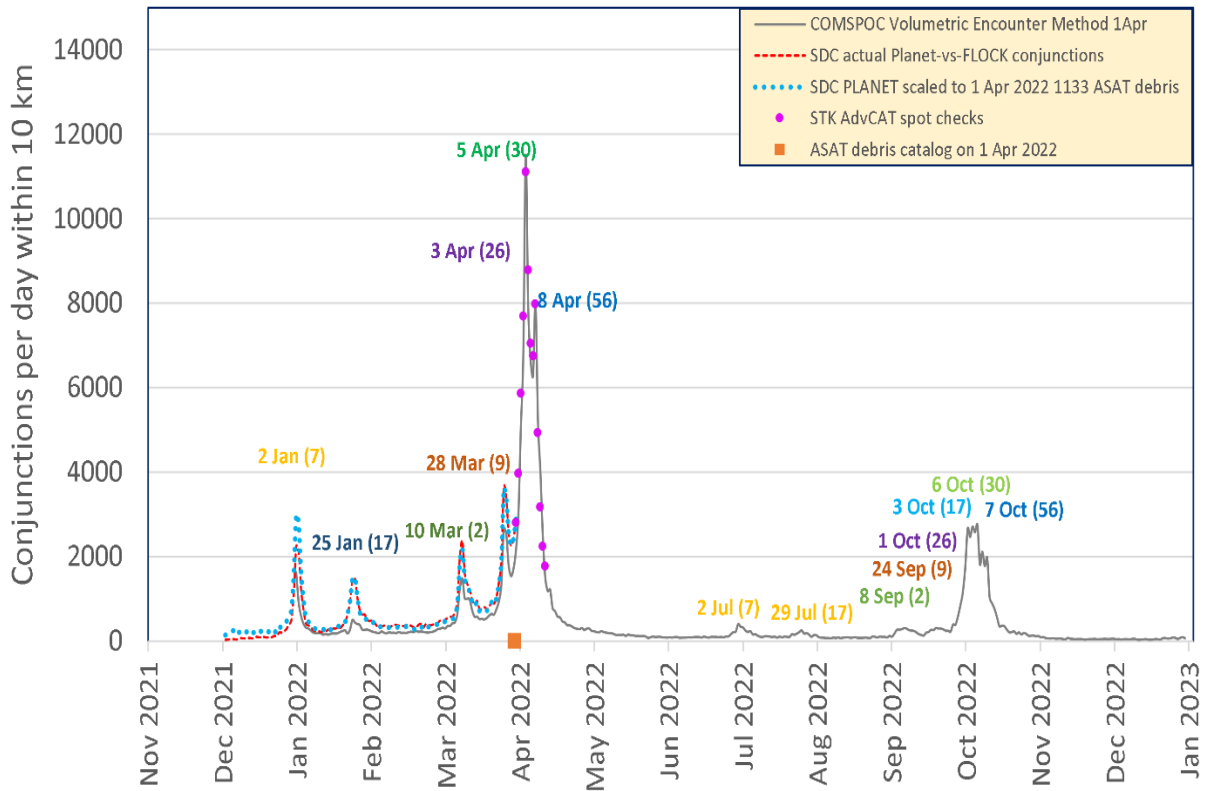


Figure 33: 1 Apr prediction of Planet conjunction rates to end of 2022.

5.1. Comparison of Planet's COSMOS 1408 encounter and collision rates versus background population

It is of interest to compare the encounter and collision rates caused by debris from the COSMOS 1408 breakup with the background population. Note that while the conjunctions within 10 km spike dramatically at the 10 am LTND crossings, actual collision risk also rises dramatically at these planar crossings.

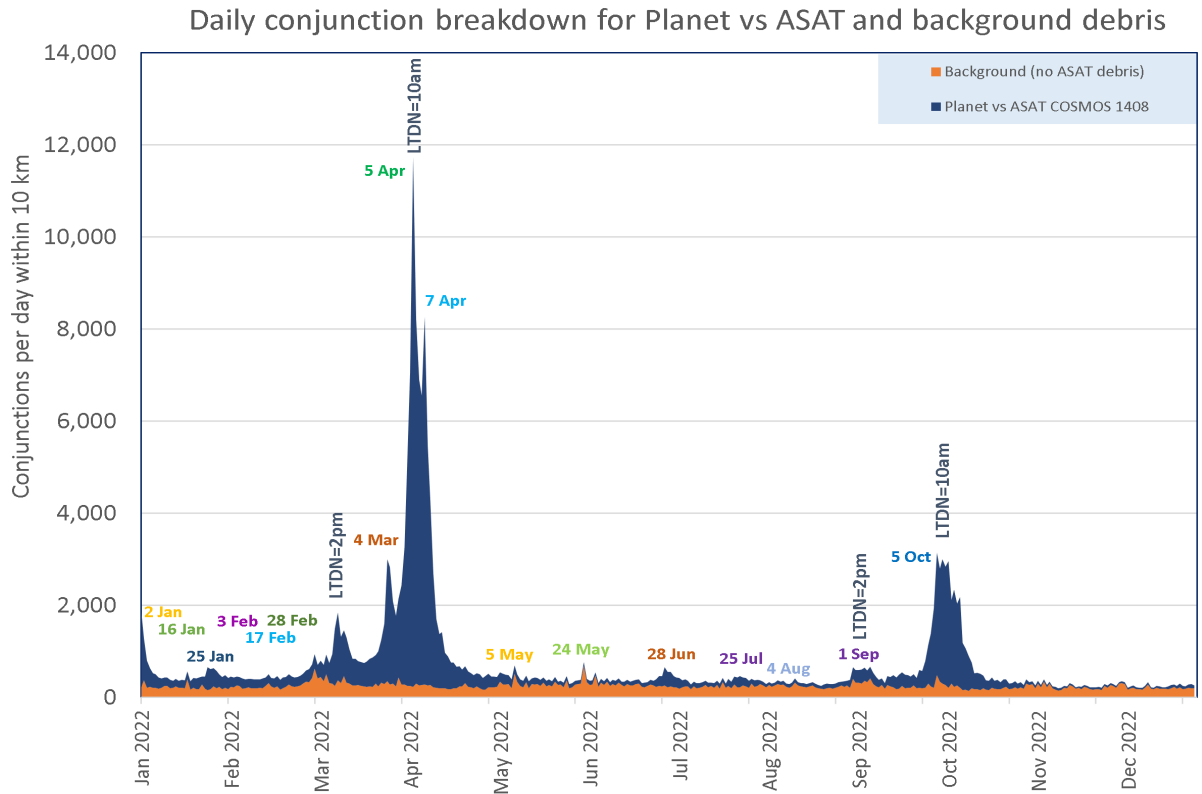


Figure 34: COSMOS 1408 10 km encounter rates compared to background rates.

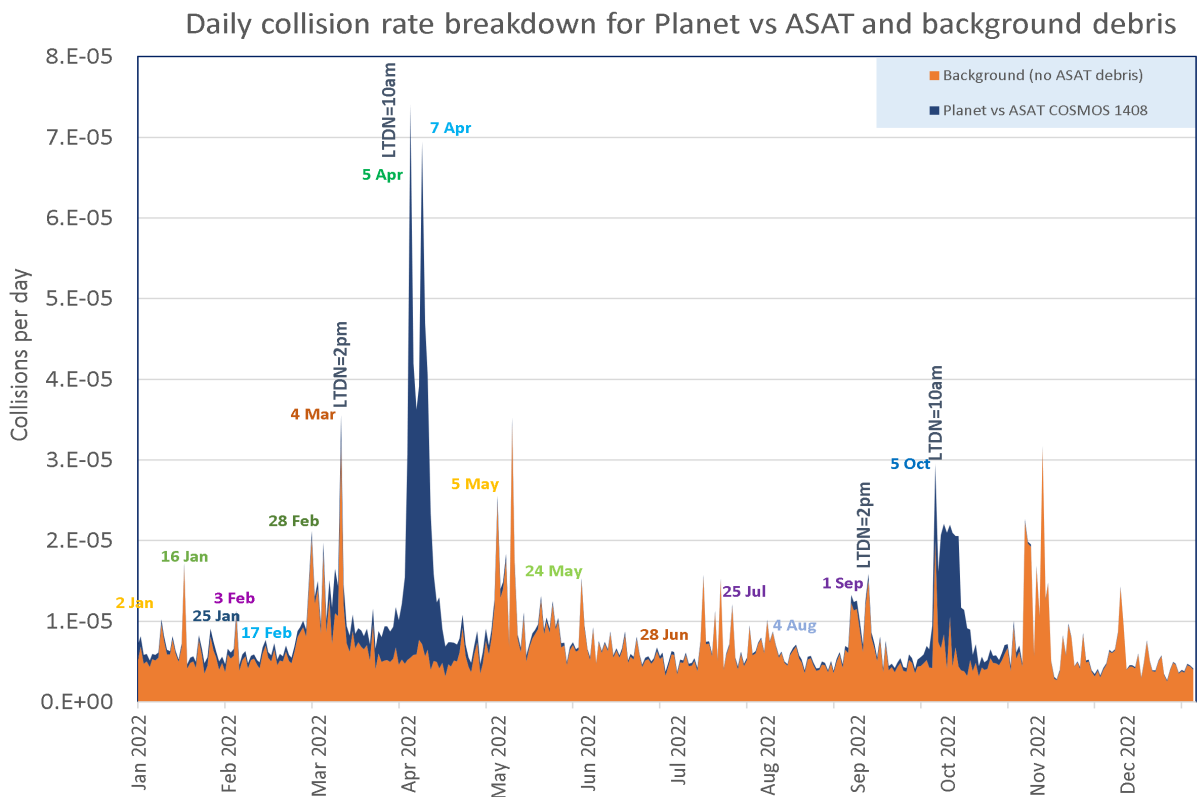


Figure 35: COSMOS 1408 10 km collision rates compared to background rates.

5.2. Encounter rate predictions for all active spacecraft

Apart from operating many spacecraft in Sun-synchronous orbits, the conjunction and collision risks facing Planet are certainly not unique to their spacecraft or constellations. A sampling of 100 Earth observing platforms spanning government, civil and commercial missions and constellations indicates very little altitudinal variation with a median altitude of 441 km at 97.8° inclination as shown in **Figure 36** and **Figure 37**.

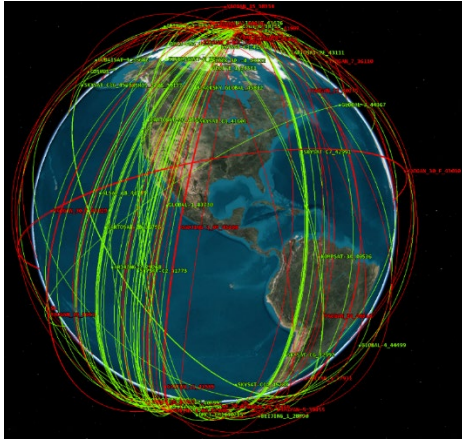


Figure 36: Sun-synchronous orbits for 100 commercial, civil & government satellites.

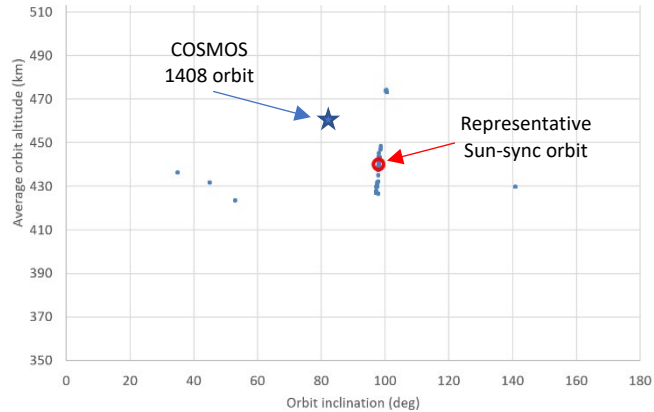


Figure 37: Average orbit altitude versus inclination for 100 Sun-sync orbits.

This indicates that many Earth observing constellations and spacecraft may face the same phasing effect first detected with the Planet spacecraft. This is noteworthy, in that there are 360 operational spacecraft with inclinations between 97.6 and 98.1° inclination, many of which are owned by PRC and the United States.

To confirm that many of these spacecraft are similarly affected, the volumetric encounter algorithm was applied to all active spacecraft for the year 2022 as shown in **Figure 38**. Many CubeSat constellations have similar close approaches.

Fortunately, the CubeSat-sized earth observing spacecraft experience a lower collision probability, as evidenced in **Figure 39**. But larger spacecraft (e.g., ISR) and large constellation spacecraft will see elevated collision risk from this ASAT test.

The International Space Station (ISS) and Starlink constellations have been adversely affected as well, as shown in **Figure 40** and **Figure 41** respectively. For the ISS analysis, the Volumetric Encounter Tool was modified to add a “pizza box” exclusion shape (50 x 50 x 4 km in total size) to the existing spherical and ellipsoidal shapes.

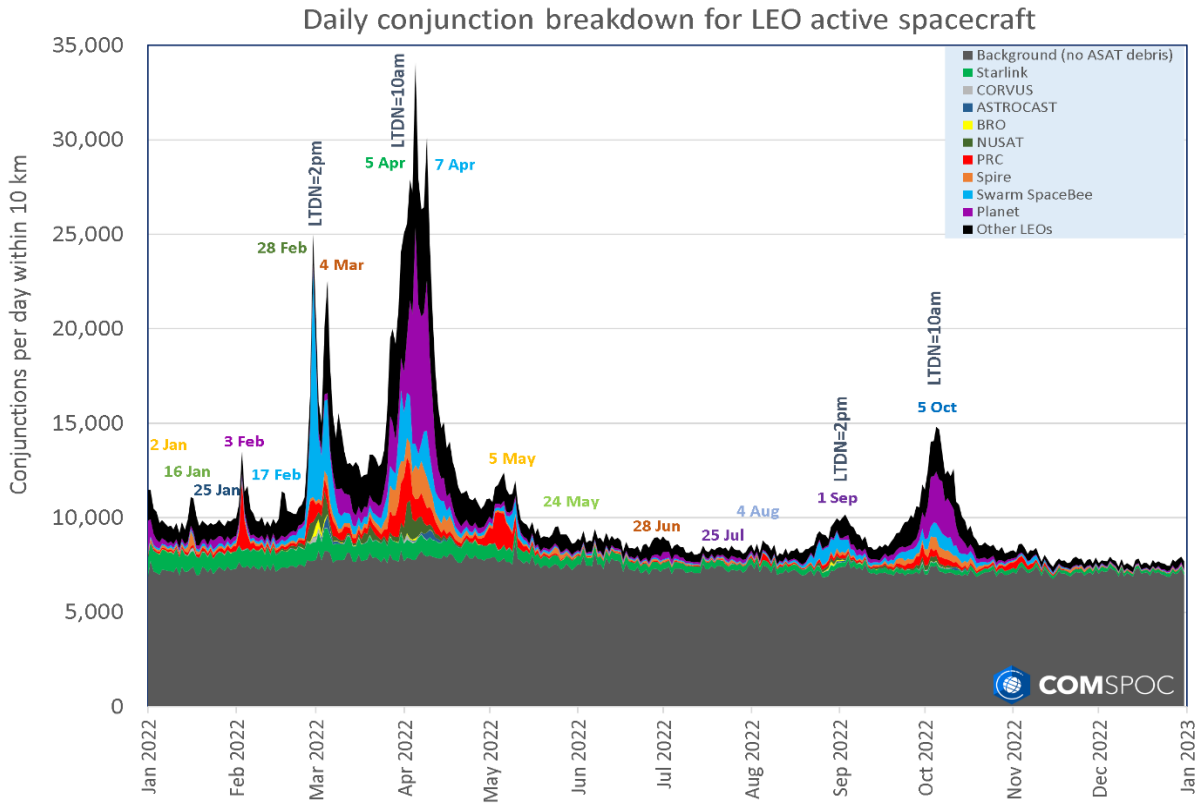


Figure 38: Conjunction squalls for active spacecraft.

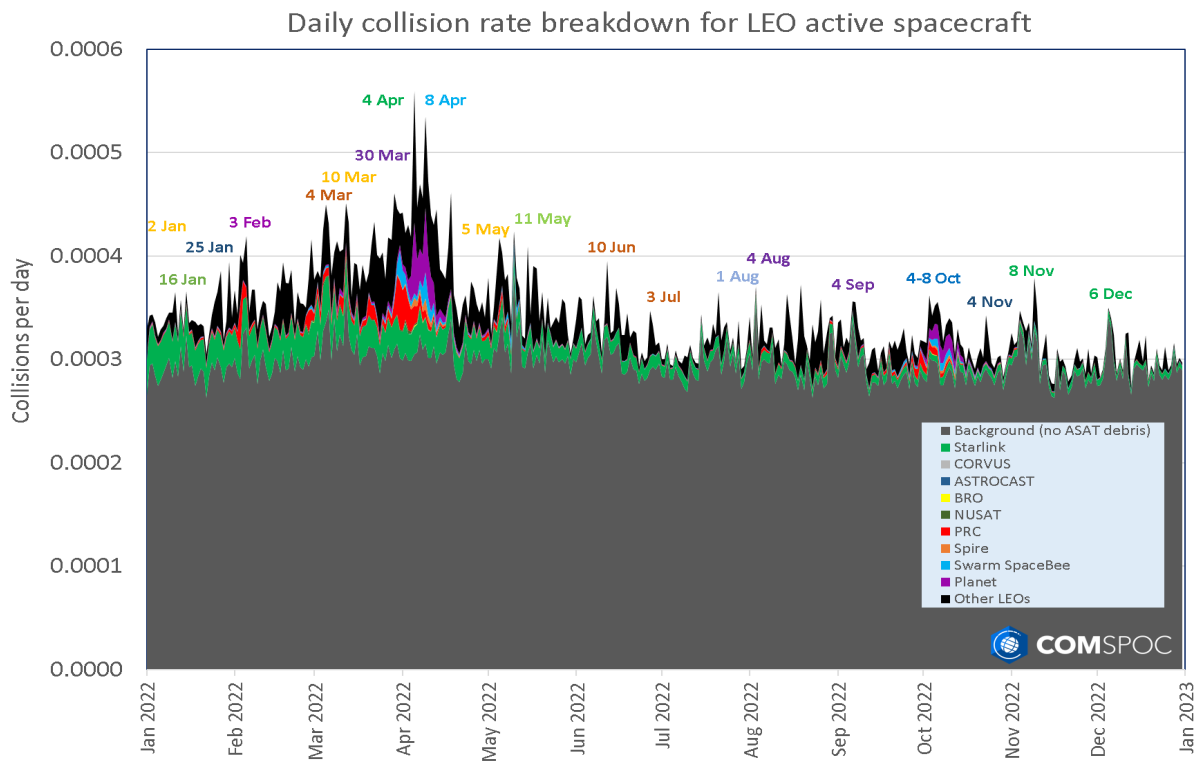


Figure 39: Collision risk for active spacecraft.

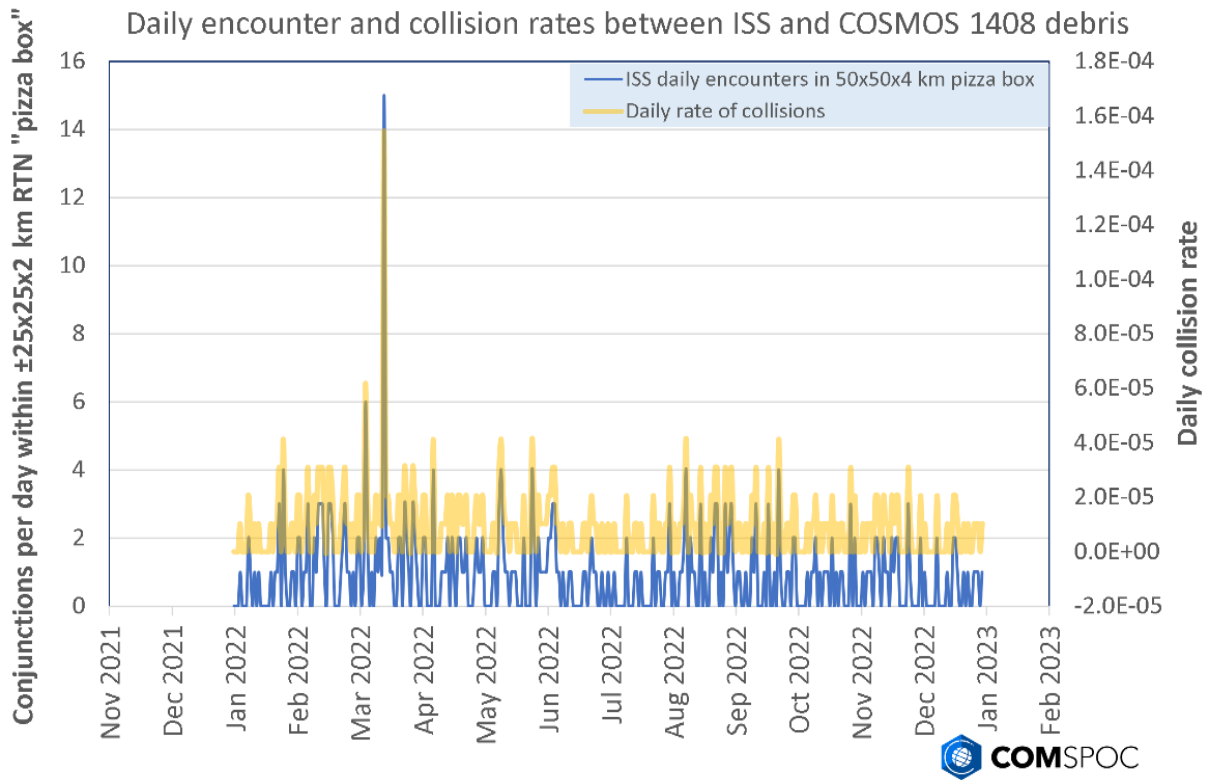


Figure 40: Encounters and collision rate for the ISS.

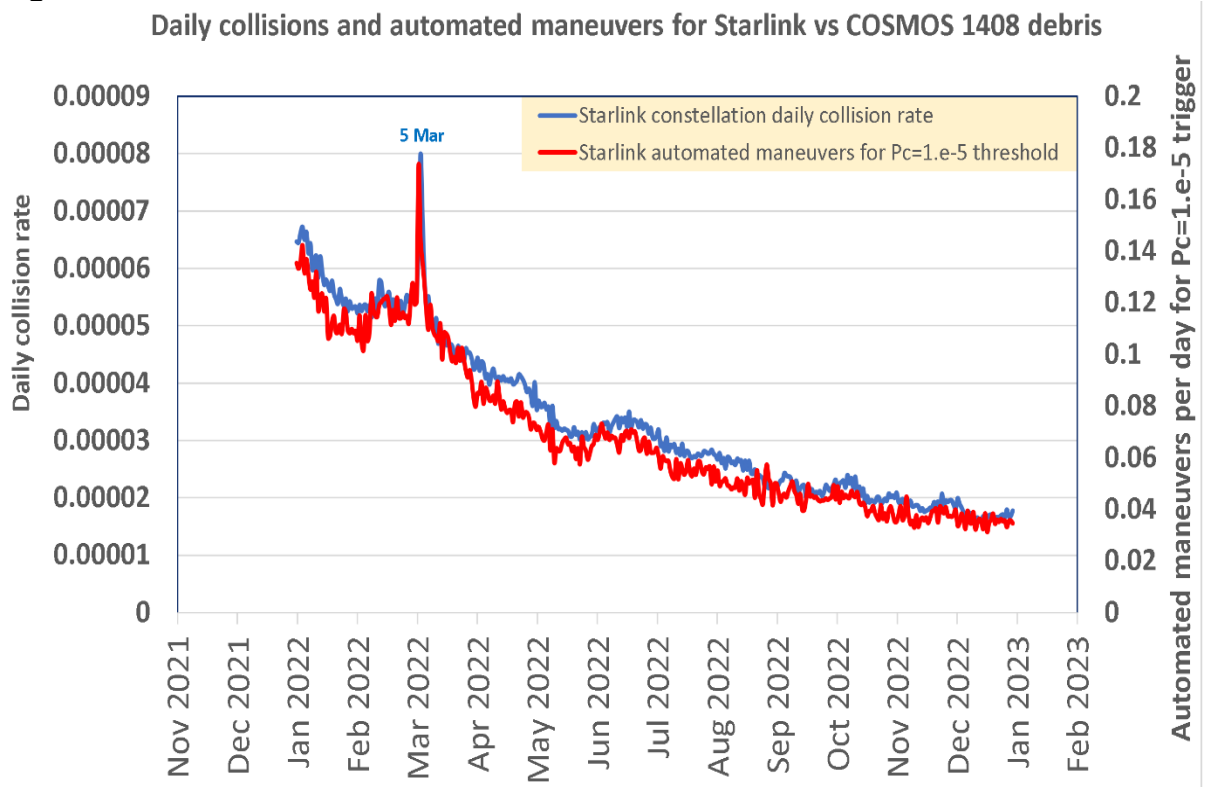


Figure 41: Estimated rate of collision and frequency of automated avoidances.

Figure 42 shows the strong band of COSMOS 1408 debris. As this band moves to the left (regresses) and Sun-synchronous orbits (thinner 'fan' of three bands at right) process to the right, the periodic 'sharing' of orbital planes leaves the debris and spacecraft in counter-rotating orbits.

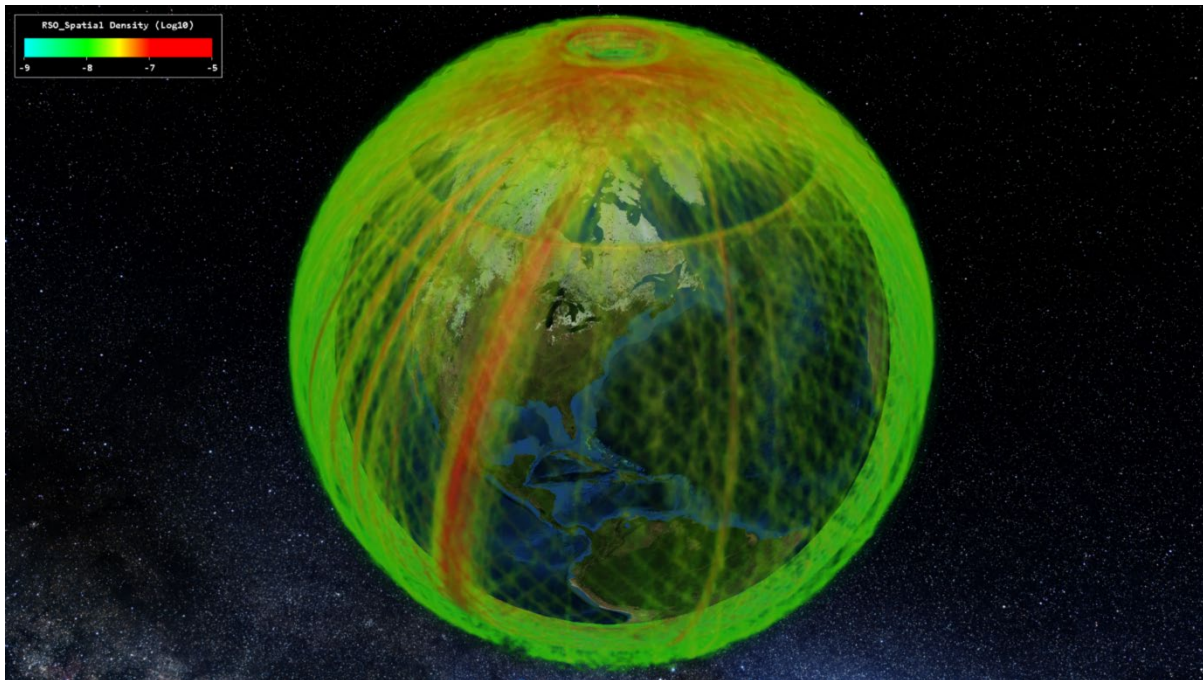


Figure 42: Spatial density of LEO space environment based upon actual tracked objects, clearly showing COSMOS 1408 debris band (lower left to upper right).

6. FUTURE WORK

We will be monitoring the conjunction situation closely this year using our flight safety systems and encounter rate assessment tools. We will compare the predictions contained in this paper with observed encounter rates and summarize our findings in an upcoming paper.

7. ACKNOWLEDGEMENT

Our thanks to the Space Data Association and Planet for allowing us to share conjunction rate data on spacecraft in Sun-synchronous orbit which initially brought this global operator and SSA Service Provider resourcing and collision risk issue to our attention.

8. CONCLUSIONS

This paper has characterized the likely intercept scenario, debris fragment ensemble and the space it occupies, spacecraft affected, and the increased operator and SSA system workloads, maneuver fuel expenditures, and collision risk.

These results indicate that operators and spacecraft have been, and will continue to be, subject to a significant increase in LEO collision risk, conjunction warnings and avoidance maneuvers, particularly so for spacecraft in Sun-synchronous orbits which are predominantly used by Earth-observing spacecraft.

We identified the presence of “conjunction squalls” affecting government, commercial SSA, and commercial spacecraft operator systems. While such conjunction squalls have already taxed flight safety systems and spacecraft operators, we predict still more dramatic encounter rate loading, avoidance maneuvers, and collision risk in the days surrounding 5 April 2022.

The team was able to employ our volumetric encounter rate software to accurately assess how frequently active spacecraft will encounter debris (for spherical, pizza box, or ellipsoidal keep out volumes), and the tool was also able to estimate collision risk that the ASAT debris poses to all constituent spacecraft.

This research provided a “trial-by-fire” opportunity for the volumetric encounter tool. Its ability to provide an accurate, forward looking, predictive risk assessment is a gap we’ve observed for not only satellite operators but also SSA and Space Domain Awareness systems. The independent verifications accomplished in this study using such operational tools as the Space Data Center, the 18 SPCS CDMs, Systems Tool Kit’s Advanced CAT (AdvCAT), and Planet’s systems are noteworthy.

From a miss-distance-based conjunction perspective, it is the CubeSat Earth observing constellations that will face the greatest increase in the number of conjunction warnings. But when using collision probability or assessing collision risk, we found that the larger (costlier) Earth observing spacecraft and large constellations such as Starlink will likely face the greatest actual risk due to their spacecraft sizes.

While orbit lifetimes are expected to be below two years for most debris fragments, we must be mindful of the additional likely thousands of Lethal Non-Trackable debris fragments that will also put spacecraft (large and small) at further risk.

9. REFERENCES

- [1] "NSSDCA Master Catalog Search" for COSMOS 1408, <https://nssdc.gsfc.nasa.gov/nmc/spacecraft/display.action?id=1982-092A>, accessed on 3 Mar 2022.
- [2] "Gunter's Space Page", https://space.skyrocket.de/doc_sdat/tselina-d.htm, accessed on 3 Mar 2022.
- [3] "The Tselina signal-intelligence satellite family", <http://www.russianspaceweb.com/tselina.html>, accessed 3 Mar 2022.
- [4] "Russia Teases New S-550 Missile System" The Moscow Times, accessed on 26 Feb 2022 from <https://www.themoscowtimes.com/2021/11/10/russia-teases-new-s-550-missile-system-a75519>.
- [5] "Database and Information System Characterising Objects in Space" (DISCOS), <https://discosweb.esoc.esa.int/>, accessed 17 Nov 2021.
- [6] The Space-Track website, available <https://www.space-track.org/>, accessed 18 Nov 2021.
- [7] Oltrogge, D.L. and Vallado, D.A., "Debris Risk Evolution And Dispersal (DREAD) for Post-fragmentation Modeling," 2019 Hypervelocity Impact Symposium, Destin, FL, USA, 14-19 April 2019.
- [8] Oltrogge, Dan. 2008. Breakup Modeling with 1Earth's DEBBIE Module and STK. Paper AGI-UTH-Oltrogge presented at the AGI Users Conference, October 7-9. Chicago, IL.
- [9] Finkleman, D., Oltrogge, D.L. Faulds, A. and Gerber, J., "Analysis of The Response of A Space Surveillance Network To Orbital Debris Events," Paper AAS 08-127, 2008 AAS/AIAA Astrodynamics Specialist Conference, Galveston, TX 27-31 January 2008.
- [10] Johnson, N.L. et al, "NASA's New Breakup Model of Evolve 4.0," Adv. Space Res. Vol. 28, No. 9, pp. 1377-1384, 2001, Published by Elsevier Science Ltd. on behalf of COSPAR.
- [11] Oswald, M., et al, "Final Report, Upgrade of the Master Model," Institute of Aerospace Systems, Technische Universitat Braunschweig, European Space Agency, Document ID: M05/MAS-FR, Rev. 1.0, Dated 26 April 2006.
- [12] Hanada, T., et al, "Low-velocity catastrophic impact on micro satellite", ESA document 2005ESASP.587..701N, 2005.
- [13] Alfano S. and Oltrogge, D.L., "Volumetric Assessment of Satellite Encounter Rates," Acta Astronautica, Volume 152, 2018, pp. 891-907, DOI: 10.1016/j.actaastro.2018.09.030.
- [14] Foster, C. et. al., "Constellation Phasing with Differential Drag on Planet Labs Satellites," Journal of Spacecraft and Rockets, Vol. 55, No. 2, 2018, pp. 473-483.
- [15] Griffith, N. et. al., "Small Satellite Collision Risk Mitigation Using Differential Drag", Proceedings of the 72nd International Astronautical Congress (IAC), Dubai, United Arab Emirates, Oct. 2021.
- [16] Rabalais, B.W., "Observed peaks in satellite conjunctions with debris populations," AMOS SSA Conference, Sept. 2013, accessed 3 Apr 2022 at https://amostech.com/TechnicalPapers/2013/Orbital_Debris/RABALAIS.pdf.